공학박사학위논문

가시광선-적외선 영역 내 능동 위장을 위한 열전 기반 인공 피부에 관한 연구

Thermoelectric System Based Artificial Skin for Active Camouflage in Visible to Infrared Spectrum

2023 년 02 월

서울대학교 대학원

기계항공공학부

설 혜 연

가시광선-적외선 영역 내 능동 위장을 위한 열전 기반 인공 피부에 관한 연구

Thermoelectric System Based Artificial Skin for Active Camouflage in Visible to Infrared Spectrum

지도교수 고 승 환

이 논문을 공학박사 학위논문으로 제출함

2022 년 10 월

서울대학교 대학원

기계항공공학부

설 혜 연

설혜연의 공학박사 학위논문을 인준함

2022 년 12 월

위 원 장 : 송 한 호 (인)

부위원장 : 고 승 환 (인)

위 원 : 도 형 록 (인)

위 원 : 강 용 태 (인)

위 원 : 권 진 형 (인)

Abstract

Thermoelectric System Based Artificial Skin for Active Camouflage in Visible to Infrared Spectrum

Heayoun Sul
Department of Mechanical and Aerospace Engineering
The Graduate School
Seoul National University

Cephalopods inspired many researchers with distinctive camouflage ability from other species which is to hide in any background readily in both infrared (IR) and visible spectrum, but this still remains a conundrum. In this study, the author developed a flexible multispectral imperceptible skin-like device that actively imitates the surrounding environment, both in IR-visible integrated spectrum only by simple temperature control in the bi-functional device. The thermoelectric layer inside the device enables thermally cloaking in the IR spectrum by controlling the outer surface temperature as surrounding accurately by cooling and heating.

This temperature variation is also adjustable to control the thermochromic layer on the outer surface of the device to produce various colors, which enables to expand the cloaking range of the visible spectrum and ultimately it provides a day-and-night stealth platform in a single device by simply controlling the temperature. Besides, independently composed scalable pixels of the device enable blending with background with a sophisticated pattern of higher resolution by localized control of each pixel and eventually enhancing the level of imperceptibility.

As a proof-of-concept, human skin can be concealed in the multispectral regime by the skin-like single device as in nature, our work is expected to contribute to the development of next-generation covert military wearable suits and to improve multispectral cloak that includes invisible gadgets in the science fiction movies.

Keywords: Thermoelectric
Camouflage
Artificial Skin
Visible-to-Infrared range
Biological Inspiration

Student Number: 2018-36896

Table of Contents

List of Figures

Chapter 1

Introduction

1.1 Study background

In nature, there are numerous camouflage skills for surviving. A number of species actively blend into the environment, mainly by changing their skin shape or colors for predation when they are hunting and defense against being attacked by prey. Thereby the probability of survival can be increased.

Cephalopods have the distinctive camouflage ability from other species, which is reflecting the visible and IR wavelength respectively, depending on its need to hide into any background by rearrangement of chromatophores in their dermal layer through the spontaneous and rapid neural and muscle signals.[1-4] Many researchers have been inspired by these camouflage abilities and researching to artificially imitate the skills since the human skin have not these active cloaking abilities despite the outstanding senses and versatile functionalities.

Especially, active imitation skill from the visible-to-IR spectrum of cephalopods have been studied since the 1800s for military purposes as the stealthtechnology which has proved to effective application for concealing or surveilling from the

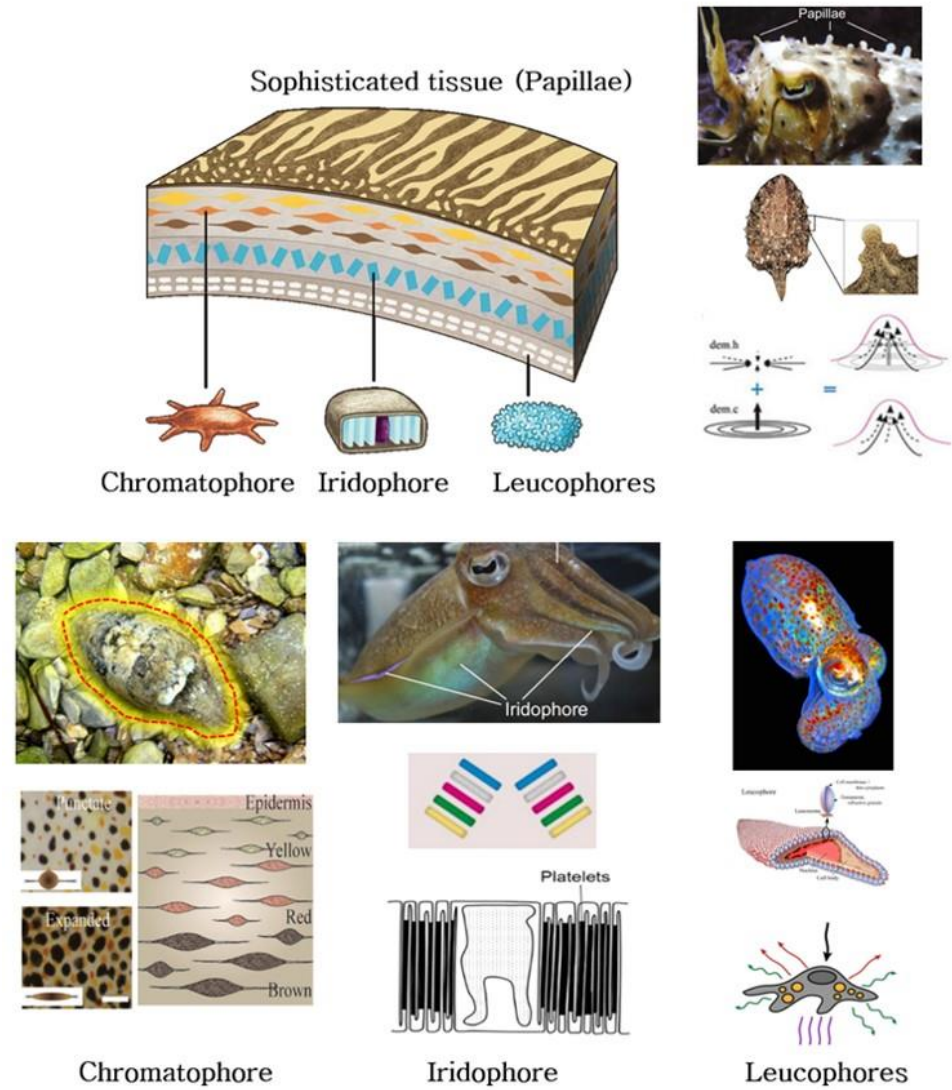

Figure 1- 1 Cross-sectional schematic of cephalopod skin showing their complex skin cells' architecture, which embedded pigment granule-packed chromatophore organs, proteinaceous microstructure containing iridophore cells, and intracellular nano sized particle filled leucophore cealls. Note that the figure shows representative camouflage skill depictions of the cephalopods. [1-4]

enemy.

Driven by these sources of inspiration, the scientists have endeavored to make a complete wearable cloak that operates in the visible-to-infrared range for a long time. Despite the lengthy effort, most of the commercialized and widely-used products are only confined to mimic the chromatic pattern, and the technology which can be actively blended into the background from visible to infrared spectrum that operates in a single device does not demonstrate yet. This means the development of an artificiallymultifunctional device that actively emulates the surrounding environment is difficult and realizing such a wearable imperceptible technology remains an engineering conundrum yet but should be studied to expand for future applications.

1.2 Previous researches

In this regard, many researchers have been challenging those inspired by the autonomous and active camouflage functionalities from cephalopods, to reconstruct the cloaking system by using the physical or electrical mechanism. However, realizing a soft camouflage wearable that operates in the full spectrum(from visible to IR) with a single device structure is a huge challenge. The imperceptible wearable that operates only in the visible spectrum would be detected by the infrared(IR) vision camera at night, and the vice-versa case would be easily identifiable in the naked eyes in daylight. Much of previous literature is utilized various methods such as electrochromic, thermochromic and mechanochromic phenomena[20, 21, 22, 23]

to alter the colors within the visible wavelength, while several researches investigated the metamaterals and electro-actuation which reflect the IR wavelength for cloaking into the IR regime or developed the temperature adjusting device to match background temperature by using the mechanism that temperature(or radiated heat) can be directly translated into the IR signals to simply mimic the IR wavelength. [6, 11]

However, most of them achieved only separately operating devices either visible or IR to imitate as the background which means it is not dual functioned in a single device structure that can readily switch between the visible an IR mode depending on a desirable situation. Recently, to the best of the authors' knowledge, Morin et al. developed the soft robot system with visible and thermal cloaking functions for the first time by controlling the fluid flow of different temperatures and colors through the microchannels inside the device.[5]

Although the novel concept succeeded to mimic the dual functionalities of the cephalopods in a single device, the microchannel system is not only extremely difficult to match the temperature and color of the fluids to the background but also has a low level of uniformity and responsivity to change to other colors or temperatures since it requires a complex procedure of absorbing and filling the microchannels with other fluids of various conditions. In addition, controlling the two independent variables, color and temperature, through the fluids as the middle transfer medium to demonstrate cloaking effects causes the complexity, inefficiency and bulk system in the soft robot. It is apparent that there are a clear need and opportunity for improvement for the imperceptible device that works for both day and night in a simpler and yet more advanced way.

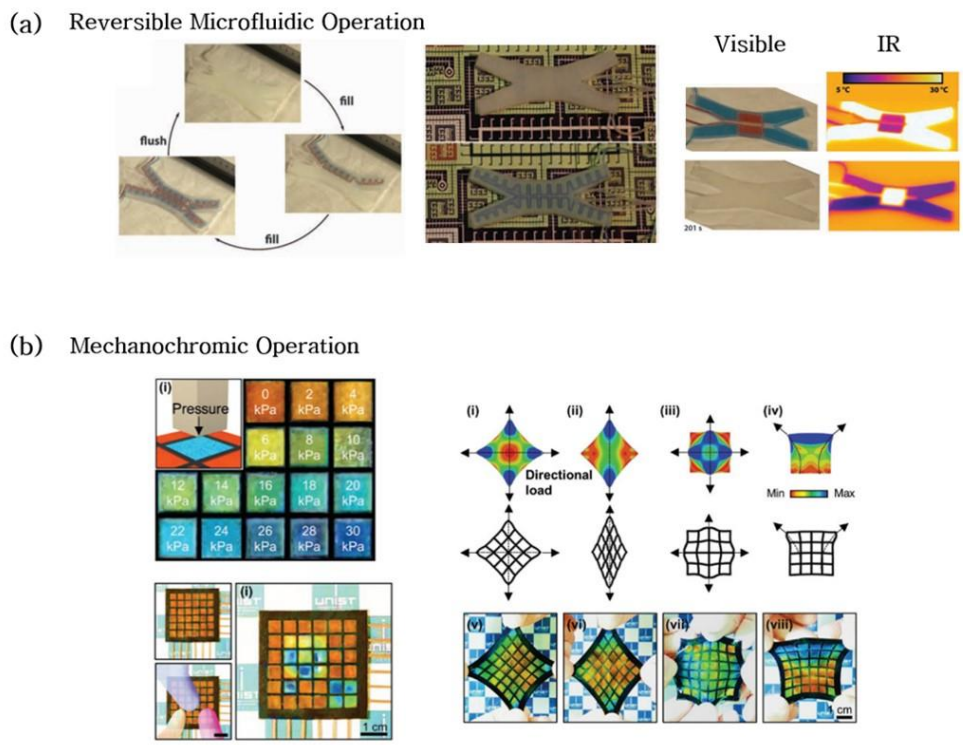

Figure 1- 2 Previously developed representative biological-inspired camouflaging devices. (a) Early suggested visible and thermal cloaking soft device by using the microfluidic channels. This device has multi-functional characteristic but unadaptable for wearable skin. (b) A wearable photonic skin device that can camouflage in a visible range of operating as mechanical stimulation. It seems compatible with human skin but only demonstrates a single function.

1.3 Objective and overview of this study

Therefore, in this study, the skin-like imperceptible cloak that allows the human body to blend into the background in the visible-to-IR range was demonstrated for the first time. Biologically inspired by the epidermis of cephalopods in nature which can cloak in the visible-infrared spectrum, an active imperceptible artificial skin that can camouflage into the surrounding environment on demand both in daylight and at night by a single device with temperature control was demonstrated.

It is quite apparent that radiated heat(proportional to temperature) can be directly translated into the IR signal, and thus adjusting the device temperature to that of the surrounding would allow IR cloaking. In this light, the soft and skin-like thermoelectric device which can actively cool down and heat up in a single device structure to conceal the human body in the IR region by controlling the temperature was developed.

The thermoelectric facilitates thermal cloaking in the IR range by matching the ambient temperature (i.e. T=Tambient) and enables compact pixelization which is individually controlled since it generates the temperature gradient (capable of active cooling and heating) through a pair of N-type, P-type semiconductors. To expand the imperceptible spectrum from the IR to visible region, thermochromic liquid crystal is integrated on the surface which expresses the various colors by changing the light reflectance based on its temperature variation. Thus it is achieved the cloaking in visible range separately by matching the surrounding colors. (i.e. R(T)=Rambient) This means, in this device structure, simply adjusting a single variable input (temperature) serves to integrate the multispectral imperceptible

system in the visible-to-IR range.

To adapt the device directly to the human skin surface as the wearable system, the frame of the device is composed of soft elastomer which has biocompatible and flexible properties. In addition, instead of consisting an extra heat exchange system to thermoelectric by improving the thermal conductivity of the elastomer extremely, the thermal performance and uniformity of the device are also enhanced, and it enables the device compact and thin to increase wearability.

Moreover, the concept of the active pixelization was incorporated into the device structure to further enhance the multispectral imperceptible adaptability in the sophisticated background. Rather than a simple imperceptible device that operates as an entire bulk and thus expresses only a single color or temperature at a time, each pixel works independently of one another so that it can adapt to the complicated and disruptive pattern of multiple colors or temperatures. Highly scalable pixelation of the device creates a platform with a high resolution by adjusting the temperature of each pixel respectively and autonomously, thus it would be extraordinarily useful when cloaking at the background of sophisticated patterns or when transiently moving from one background to another,

Finally, to construct its practical platform for the imperceptible artificial skin, the thermal display is fabricated with an array of several pixels that delivers a variety of optical information, and scrutinized its multispectral cloaking performance using both optical an IR visions on the human skin surface. The previous work so far only suggested conceptual works or merely examined the device potential not in the form of the complete working device that can be directly worn on the human body. In this

regard, unlike the previous devices, the device that developed in this study takes a form of a totally functional cloaking wearable system that completely conceals the human body in the full spectrum while directly conforming to the deformable surface of the human body.

Based on the results, it is anticipated that this new type of artificial imperceptible

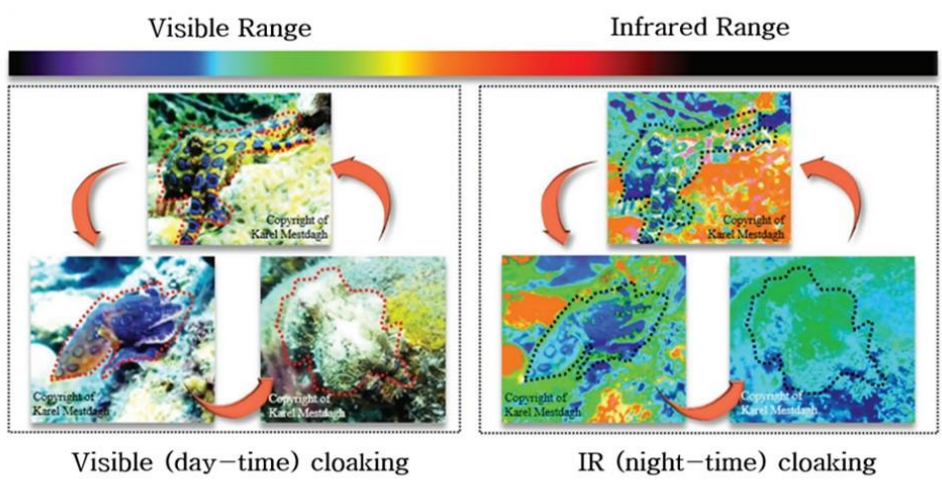

Figure 1- 3 Snapshots of cephalopod under the visible-to-infrared spectrum. This indicates the instantaneous camouflage ability of cephalopods to blend into the background by autonomous rearranging the multi-layer of the dermis. It enables conceal its figure in the visible wavelength and IR range since multi-layers of cellular lamellae that are composed of chromatophore, iridophore, and leucophore function as the Bragg reflector that reflects the broad-band wavelengths of light by biological synaptic signaling. [7]

skin-like device, which operates in the full spectrum just by controlling temperature in the single device architecture, would contribute substantial implications to the stealth military applications in the imminent future. Furthermore, it is expected that the device would become meaningful assets for the development of the complete invisibility gadgets, perhaps suggesting that these gadgets from the classic science fiction movies may not be of surreal imaginations any longer. Considering the functional advance and practical implications of this work, this study has enough significance to become a foundation of multispectral wearable camouflage device.

Chapter 2

Preparation and Method

2.1 Material Preparation

The system consists of several pairs of thermoelectric semiconductors as the temperature variation producing media, highly thermally conductive elastomer for uniform heat spread which also supports the outer frame of the device, and thermochromic ink that can be responded and varied its color by temperature change.

The P, N type thermoelectric pellets (Wuhan Xinrong New Materials) were soldered on the Cu film electrode exposed surface which is avoided the elastomer frame at 220 ℃ for 20 minutes under mechanical pressure in N2 atmosphere to prevent oxidation of the electrode. The counterpart electrode also soldered on the other side of thermoelectric pellets utilizing the same process.

To comprise metallic fillers in the highly thermally conductive elastomer(HTCE), various materials which have different structures such as silver flake(Sigma Aldrich), synthesized silver plate and EGaIn (Alfa Aesar) were incorporated. EGaIn was oxidized by stirring with acetone for 24h since Ag and Ga in EGaIn have the potential to react and make the alloy. This oxidation process alters the outer surface

of Ga to Ga2O3 which has low possibility to react with Ag.[8][9]

The silver plate was synthesized as following procedure: First, blend the 0.0849 g of AgNO3 (Sigma Aldrich) in 0.5 ml of DI water and prepare dissolved 0.25g of PVP (Sigma Aldrich, 36k MW) into 5 ml of DI water in a separate vial. Second, mix the PVP solution and AgNO3 solution with additional 39.65ml of DI water under stirring condition. Third, mix 0.0117 g of NaCl (Sigma Aldrich) in 2 ml of DI water and pour it into the solution which was made in 2nd process. As the last step, 1.15 ml of H2O2 (Junsei Chemical Co., Ltd) is poured into the 3rd mixture and then add diluted ammonia hydroxide (1.282 ml NH4OH + 0.418 ml DI water). After stirring gently for 30 min finally synthesizing the silver plates completes.

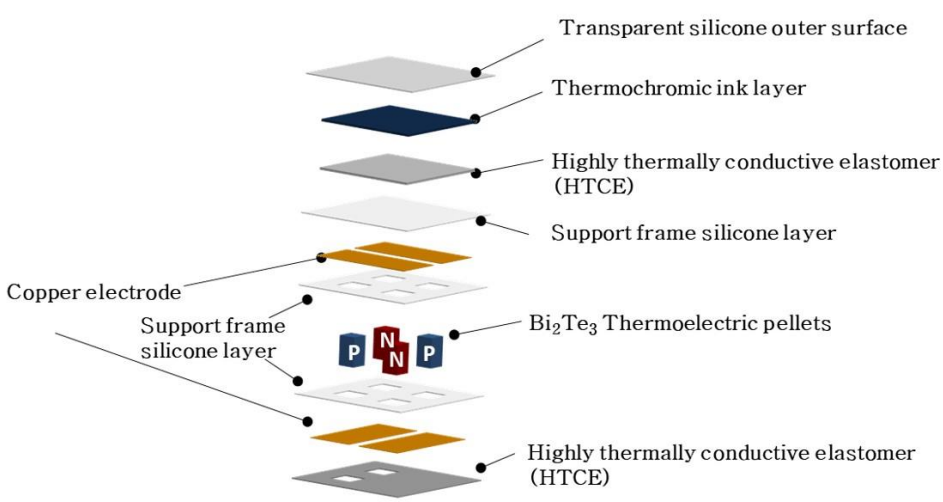

Figure 2- 1 3D visual illustrations of the device comprising thermochromic ink, Cu electrode, ahighly thermally conductive elastomer, and thermoelectric pellets, which are connected in series.

3 types of fillers(silver flake, oxidized EGaIn, silver plate) are ready, and to make the metal-based elastomer oxidized EGaIn and silver flake were mixed into Ecoflex (Smooth-On 00-03) in the respective weight ratio of 3.5:3.5:3 until the homogeneous mixture is achieved. Then, spin-coat the mixture at 500 rpm for a minute and cure it at 60 ˚C for 10 minutes. After fully cured, the silver plate was vacuum-transferred onto the metal-based elastomer mixture and repeat this spin-cast and vacuum filtrating process until the HTCE takes a form of three silver plate layers are inserted into the three metal-based elastomer mixtures.

In this structure, silver plate layer generates the high in-plane thermal conductivity and electric conductivity of HTCE through the stacking of overlapped plate form of silver which has high thermal and electric conductivity. On the other hand, despite metal-based elastomer is composed of electrically conductive liquid metal(EGaIn) and silver flake to improve the thermal conductivity, remains thermally improved but electrically insulating because of Ecoflex. Consequently, by encapsulating the silver plate layer with the metal-based elastomer, electrically insulating yet highly thermally conductive elastomer completes.

On the outermost surface of the HTCE, the light-absorbing ink(Kenis, Japan) mixture with Ecoflex was spin-casted and cured slowly to make the flat-coated surface, after then thermochromic ink (SFXC, cholesteric liquid crystal ink) was subsequently spin-casted on it.

2.2 Fabrication Process

The simplified schematics of the fabrication process are shown in figure 2.2. First, shaping the HTCE according to the designed geometry of the pixels by using the laser-cut without peeling off the remaining HTCE. Then, subsequent laser-ablation(Nanio Air 355-3-V, Innolas, λ=355nm) of the 25 μm-thick Cu film (Alfa Aesar) on the HTCE would fabricate the cu electrode on one side. After removing the rest part of the Cu film, spin-case Ecoflex on the Cu electrode and HTCE at 1000rpm for 30s and cure it at 60 ˚C for 10 minutes. To expose the contact part with the thermoelectric pellet, circular holes of Ecoflex are laser-ablated and carefully peeled off.

The Bi2Te3 based P-type and N-type thermoelectric materials(LG innotek) were diced into W1.5 mm x D1.5 mm x H2.5 mm and were soldered in the alternating order onto the exposed part of the Cu electrode at 230 ˚C for 10 minutes under N2 atmosphere to prevent oxidation of the electrode. In the results of the previous study which is conducted by the author, the interfacial delamination between the Cu electrode and thermoelectric pellets became a cause of mechanical failure under fatigue stress. Also, thermal performance was decreased since the thermal resistance at the contact area as heat junction was increased extremely. At the embryonic stage of the research, the commercial silver paste and conductive epoxy were employed to adhere the Cu electrode to the thermoelectric pellet, but the adhesion strength of these materials was so weak that delamination occurred under strain. In contrary, Pb40Sn60 soldering, however, creates an intermetallic layer with Cu as Cu dissolves into molten Sn to form Cu6Sn5 and Cu3Sn, which serves to constitute a relatively strong bond between two interfacial layers.[34] Thus, in figure 2.3., the

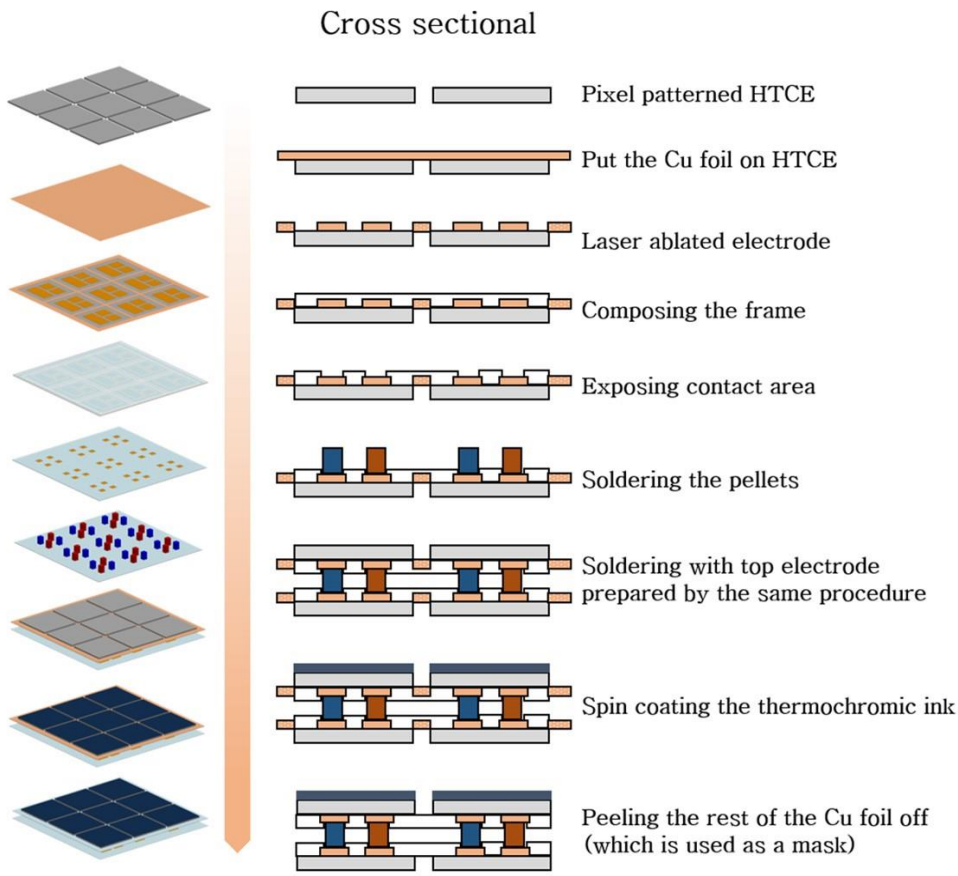

Figure 2- 2 Simplified schematic representation of the cloaking device fabrication procedure.

experimentally conducted results of bonding strength which compared to other bonding agents showed that in case of soldering the fracture of the Cu electrode rather than delamination of the Cu electrode from the thermoelectric pellet is more likely a reason for the mechanical failure of the device under the repetitive cycles of stress test.

The counterpart (bottom part of the device) electrode is also produced as the above process on the bare HTCE with considering the electric path through the thermoelectric pellets array, depositing another layer of HTCE, making the exposed surfaces and finally soldering it with the pellets which in the fabricated part earlier.

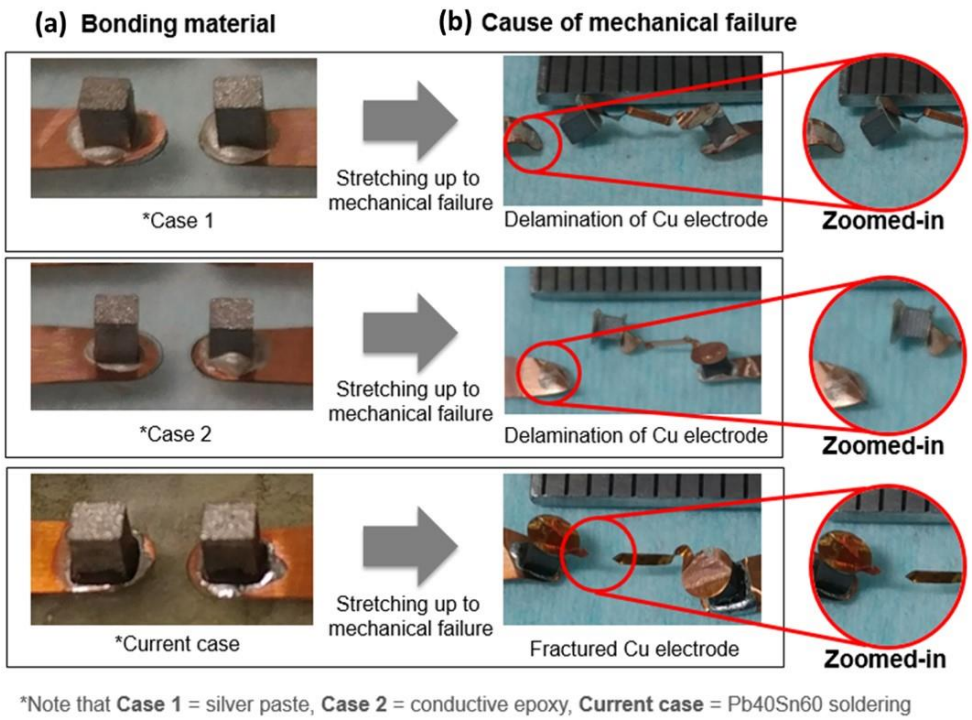

Figure 2- 3 The cause for mechanical failure after stretching for different bonding materials. (a) Image of thermoelectric pellets bonded to Cu electrode using different bonding materials (b) Images of mechanical failures for each treatment after maximum stretching. Note that the reason for the mechanical failure was delamination between the Cu electrode and the thermoelectric pellet for conductive epoxy and silver paste while it was the mechanical fracture of the Cu electrode for soldering.

To form the uniform light-absorbing layer, black ink (Kenis, Japan) is spin-casted at 1000rpm for 30s on the pixel-patterned side of the HTCE film and dried for 20 min at the RT.

Finally, the device is completed after thermochromic ink (SFXC, cholesteric liquid crystal ink) is subsequently spin-casted at 500 rpm for 60 s, and PDMS is deposited on the outer-most surface to encapsulate the device by spin-coating at 1300rpm for 30s, and removing the HTCE which in the outer frame of the pixels.

2.3 Measurement and Analysis

The figure 2. 4(a), (b). shows the experimental setup of the IR camera (FLIR A645 sc) which is utilized to obtain the temperature profile characterization of visualized thermal images that generated by thermoelectric operation by using the DC power supplies. The simplified electrical circuit illustration of the PID control system of the device to demonstrate the real-camouflage situation is shown in figure 2. 4(c).

To control the thermoelectric current condition (heating/cooling and reverse active mode), the Arduino kit was programmed. When examining the reliability of the device through the cyclic bending test, the resistance change was measured with the source meter (Keithley 2400) and the lab-made automated cyclic motion controller. The thermal conductivity of HTCE with different loading of metallic filler conditions (0 wt.%, 25 wt.%, 50 wt.% and 70 wt.%) was measured with transient hot-wire method. To verify the accuracy of the result, the laser flash apparatus (Netzsch LFA

(a) Experimental setup in real application : Heating

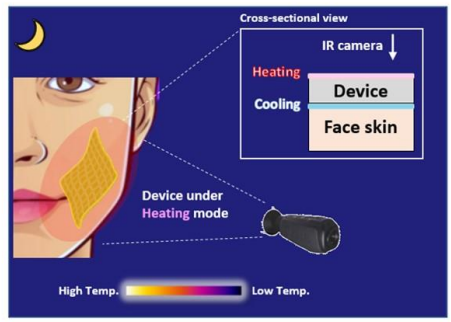

(b) Experimental setup in real application : Cooling

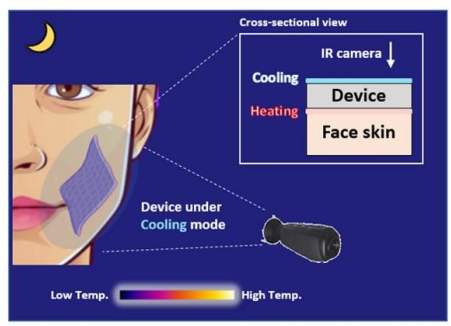

(c) Schematic diagram of electrical circuit

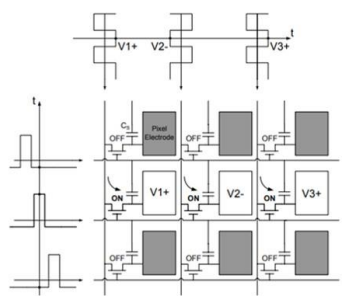

Figure 2- 4 An experimental setup for night-time camouflage with IR view of (a) the heating and (b) cooling mode on skin. Note that the heating mode of the device appears as it is cooling the skin surface and the same applies to the cooling mode. (c) A simplified electrical circuit illustration for individual control.

467) and differential scanning calorimeter (DSC204 F1 Phoenix) are used for estimating the thermal diffusivity and heat capacity data respectively since the thermal conductivity can be calculated by multiplying the thermal diffusivity, density, and heat capacity of the material.In this regard, many researchers have been challenging those inspired by the autonomous and active camouflage functionalities from cephalopods, to reconstruct the cloaking system by using the physical or electrical

Chapter 3

System Design and Optimization

3.1 Schematic and operating mechanism

Despite the difference in mechanism of multispectral cloaking, the studied device herein comprise figure 2.1 can demonstrate the considerable cloaking functionalities like cephalopod dermis. Figure 3.1 represents each pixel that consists of the bi-functional TE operation unit, which can cool and heat up by applying a reverse electric current independently, thus facilitating the accurate thermal control of every pixel. The precise control of temperature in each pixel enables the color change from red, green to blue depending on device temperature through the thermochromic layer. Meanwhile, this temperature change of each pixel also enables IR cloaking by adjusting to the radiated heat of the surrounding. Thus, despite the mechanism difference, the proposed device completes the multispectral cloaking system only with a single input variable(temperature) by integrating from IR to visible spectrum into one full spectrum in a single device. In addition to chromatic and thermal control, separated pixels facilitate the deformation and various curvatures to conform skin-like structure of the epidermal surface and therefore enable the device to be worn as the artificial skin. This new type of cloaking system should be recognized in value

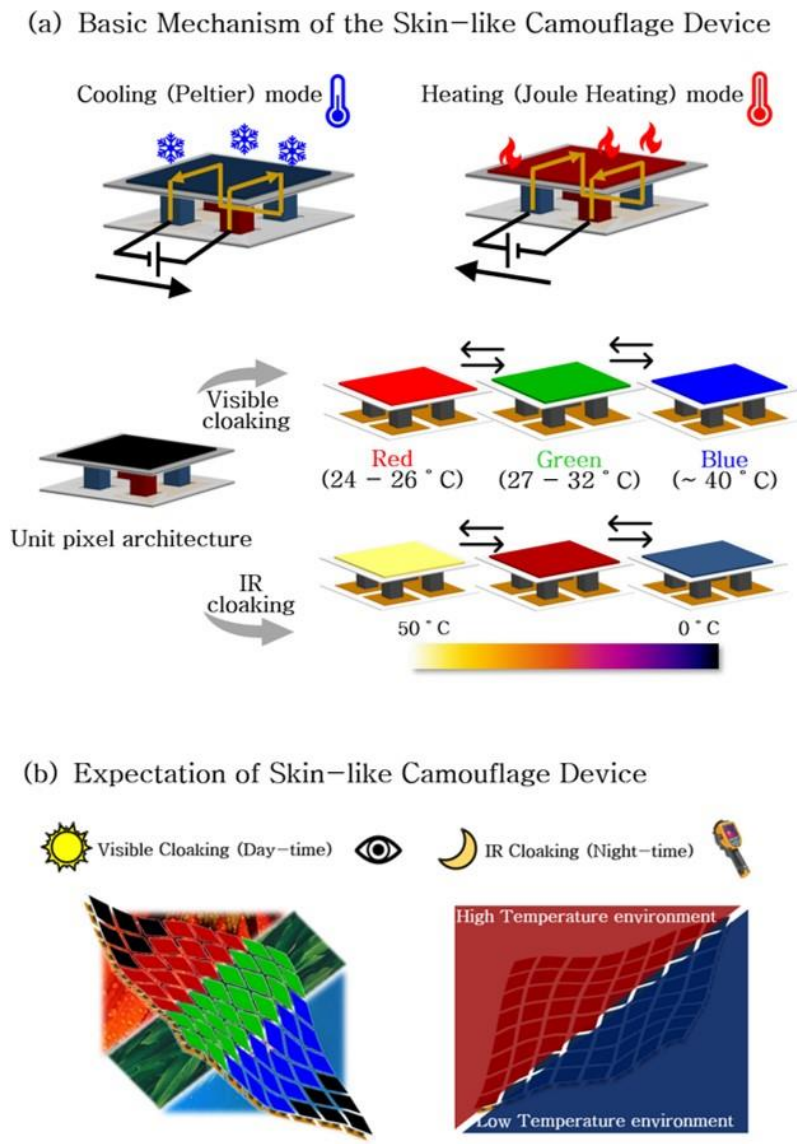

Figure 3- 1 Schematic representation of the device (a) A Single unit schematic that shows the device can actively cool down or heat up to camouflage in the multispectral(visible-to-infrared) spectrum. (b) Simplified illustration of the pixelized assembly thermoelectric device.

that it allows two separate spectrums cloaking in one device at a time even using a simple input variable to operate two different spectrum cloaking.

3.2 Thermoelectric semiconductor

To optimize the performance of the thermoelectric system, material selection and examining the geometric effect was considered on a preferential basis. The figure of merit of thermoelectric material is determined as the ZT value which is composed of temperature-dependent factors of Seebeck coefficient, electrical conductivity, and thermal conductivity. The Seebeck-Effect the main phenomenon between thermal and electrical energy conversion, is generated when there is a temperature gradient in material, because of this thermal energy the electron and electron hole are diffused and an electrical potential is buildup. The ZT value is increased with the square of the Seebeck coefficient, with temperature and electrical conductivity while it decreases with the thermal conductivity. This refers to an intrinsic property of materials and because it varies widely as temperature changes and has nonlinear relation with temperature tendency, the material selection in accordance with the purpose and operating temperature condition is important. Figure 3.2 indicates ZT value for several thermoelectric materials as a function of a wide temperature range, Bi2Te3 alloy exhibit higher ZT values near room temperature. Considering the working temperature of the device that operates on the skin surface, Bi2Te3 alloys were selected to optimize the performance and conversion efficiency in this study.

$$Z = \frac{S^2\sigma}{k}$$

S : Seebeck coefficient (dv/dT)

σ: electrical conductivity (S/m)

κ: thermal conductivity (W/mK)

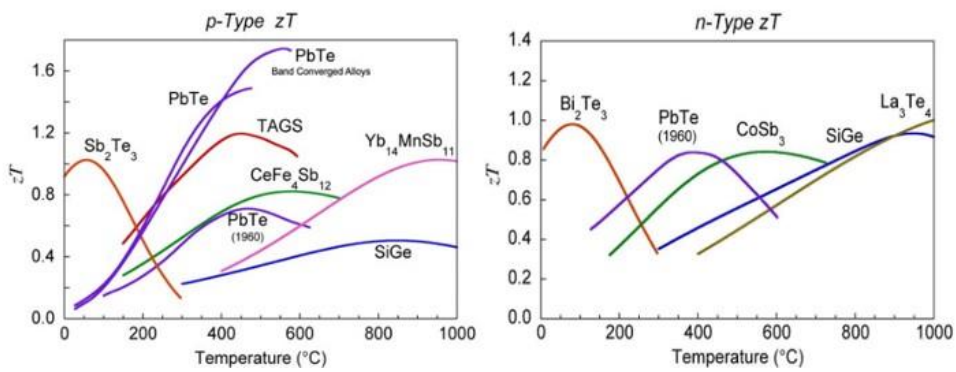

Figure 3- 2 The effect of temperature on figure of merit (ZT value)of p-type and n-type thermoelectric materials.

3.3 Optimizing the Design Parameters of Thermoelectric Pellets

Based on the Bi2Te3 thermoelectric pellet, the effect of the dimension of pellets on performance was analyzed to determine the geometric parameter of the device.

Referring to the results of the previous study, since the optimum cross-sectional area of identical height and boundary condition exists with increasing electrical current, considering performance and enough area to solder the dice to the interconnecting Cu electrode, the cross-sectional area of the leg base as 1.5mmx1.5mm was fixed.[10, 17]

Therefore in this study, to verify the effect of the pellet height on performance was numerically simulated and experimentally considered. Figure 3.3 shows the result of the cooling performance as increasing the input current for various heights of pellets. Because the cooling process is much more challenging to achieve by Joule heating effects that counteract the cooling ability as explicated in below

$$Q_c = \alpha I T_c - k\Delta T - \frac{1}{2} R_e I^2 \quad \text{for the cooling mode}$$

$$Q_h = \alpha I T_h - k\Delta T + \frac{1}{2} R_e I^2 \quad \text{for the heating mode}$$

where the first term in the parenthesis signifies thermoelectric cooling/heating (α, I, Tc, or Th stand for the Seebeck coefficient, electrical current, and temperature of the cold/hot junction respectively), and the second term represents heat transfer between two junctions (k, $\triangle$T stand for thermal conductance of the thermoelectric pellets and temperature difference between two junctions respectively). Lastly, the third term indicates Joule heating and its sign convention varies according to the cooling/heating mode.

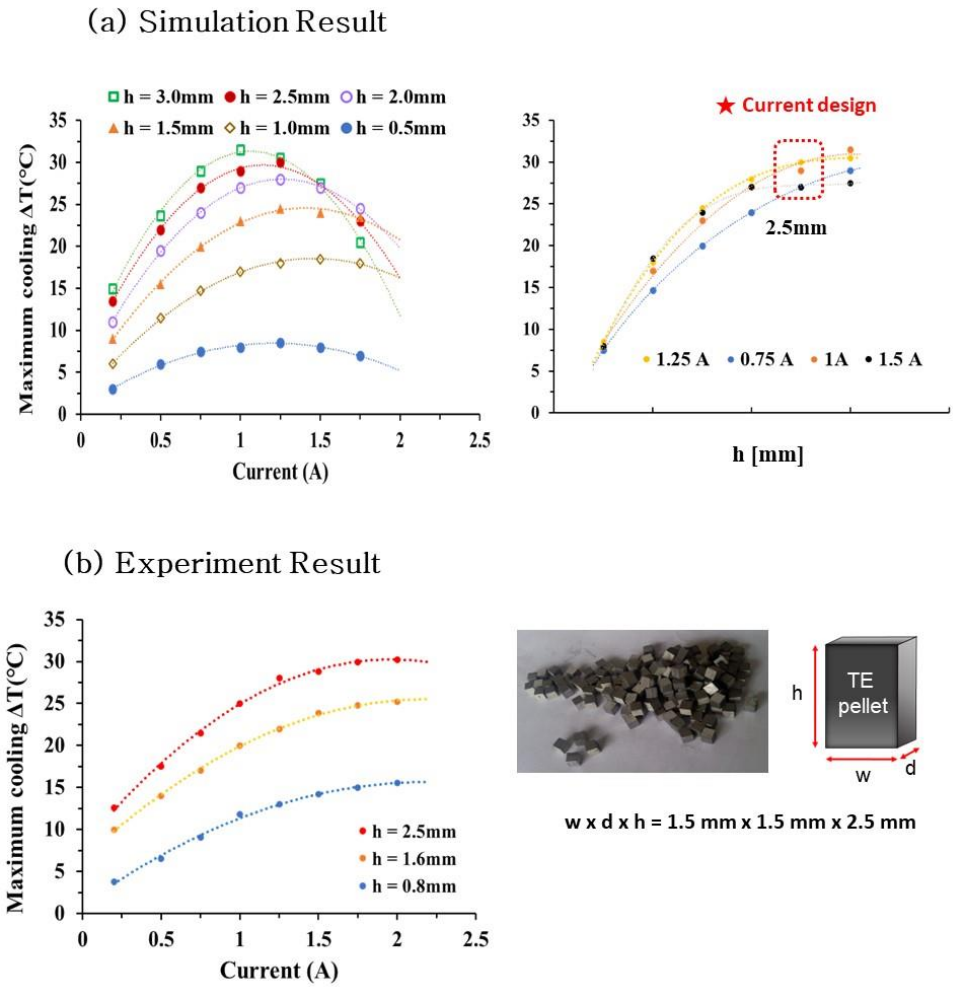

Figure 3- 3 The effect of the thermoelectric pellet height on performance.

(a) Numerically simulated result. (b) Experimentally conducted result.

The result indicates the cooling performance generally demonstrates a parabolic relationship as increasing electrical current because the effect of Joule heating overtakes the cooling performance after the optimum range of current input.

Furthermore, the cooling capacity of the device is increased as the height of the pellet leg increases, which implies that increasing the height of the pellet caused the reduction of heat conduction through the pellet because the heat bridge is extended. This phenomenon begins to converge after a certain height (h=2.5mm) with the increasing leg height because it would lower electrical conductivity. Based on this result, in addition to the cooling capacity, considering the rigid nature of the pellet and reliability such as bending stiffness and wearability, in this study optimal pellet height is set as 2.5mm.

3.4 Highly Thermally Conductive Elastomer

In this study, since the human's sense of vision as a research target object is extremely susceptible, the uniformity of the outer surface of the pixel is critical. Therefore, the external surface of the device should be highly thermally conductive to enhance heat dissipation for the realization of the exact and rapid temperature response. However, the elastomer PDMS has the characteristic of high biocompatibility and stretchability but particularly low thermal conductivity. For this reason, enhancement of thermal-conductivity is inevitable, and the selective thermal engineered device structure contributes to improving the cooling and heating performance by adjusting the thermal properties of material components. To identify the thermal uniformity of pristine elastomer, a numerical simulation based upon Ansys was conducted and the boundary conditions and results are shown in figure 3.4. As expected in figure 3.4.(a), it was figured out that the temperature distribution of the pixel surface is irregular because of the low thermal conductivity of the

(a)

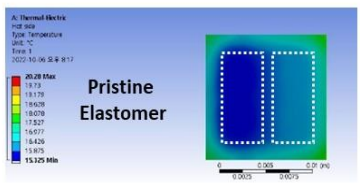

(b)

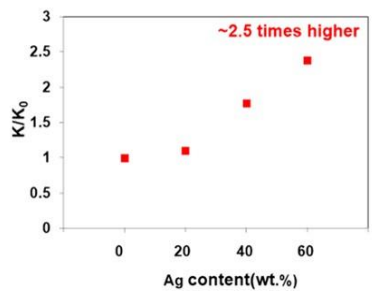

(c)

Thermoelectric materials		P type	N type	unit
Thermal conductivity	k	1.4	1.4	W K-1 m-1
Seebeck coefficient	S	215	-215	μV K-1
Electrical conductivity	σ	1050	1050	S

Elastomer properties		Pristine ecoflex	AFE	unit
Thickness		300		μm
Thermal conductivity	k	0.2	1.2	W K-1 m-1

Copper electrode		Serpentine deisn		unit
Width and Thickness		W 600	t 25	μm
Thermal conductivity	k	401		W K-1 m-1
Isotropic Resistivity	ρ	1.694E-08 (at 20°C)		ohm m

(d)

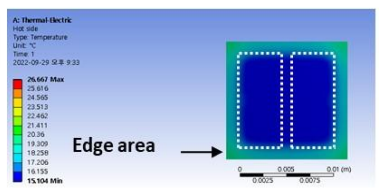

Figure 3- 4 The effect of the thermal conductivity of elastomer. (a) Numerical simulated result of pristine elastomer. (b) Thermal conductivity measurement result of elastomer as concentration which is incorporated with Ag flake. Note that thermal conductivity is improved 2.5times higher than base property. (c) Boundary condition for numerical analysis. (d) Thermal uniformity verification of thermally enhanced elastomer by numerical simulation.

elastomer. Refer to previous study by author, Ag flake were incorporated into the elastomer to boost its thermal conductivity and 2.5 times increased result were measured at 60wt% of Ag content. Considering this result on the numerical simulation, as shown in figure 3.4.(c) thermal uniformity of the central area is enhanced but the temperature contour remained at the edge (outside of the electrode) of the pixel.

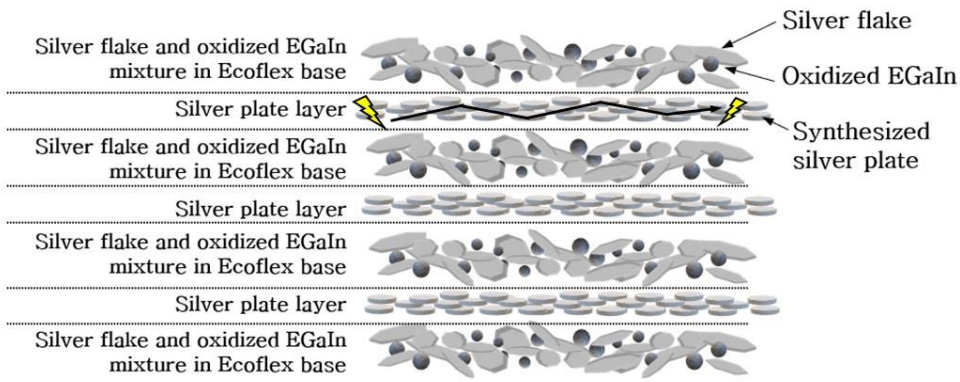

Figure 3- 5 Material schematics of the highly thermally conductive elastomer (HTCE). Note that synthesized silver plate is electrically conductive in the in-plane direction and thereby the structure possesses highly anisotropic electrical conductivity in the in-plane direction. However, since the shearing mixing layer of silver flake and oxidized EGaIn and ecoflex is not electrically conductive but thermally conductive, it is electrically safe on human skin.

For this reason, to increase the performance, combining various metallic fillers of different forms and arranging these fillers to the lateral direction and staking it as a multi-layer enhance its thermal conductivity when compared to the base elastomer. (details are explained in figure 3.5) Even though the HTCE film used in this device is composed of a multi-layer, it is fabricated only a few hundred micrometers thin.

Figure 3.6 demonstrates the thermal conductivity and stretchability measurement result of HTCE. The in-plane thermal conductivity of HTCE with 70 wt% of metallic fillers and layer is almost 8 times enhanced than that of base elastomer. Based on this result in figure 3.6.(b), numerical simulation was also analyzed and the result showed a fully stabilized temperature throughout the whole surface area. Figure 3.6.(c)

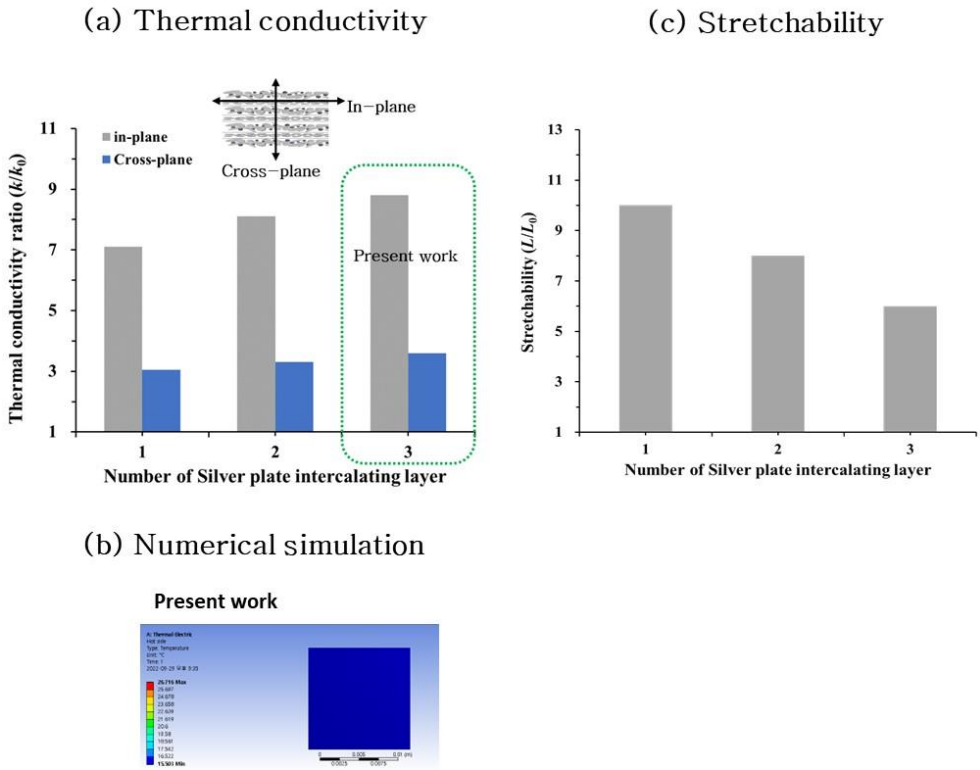

Figure 3- 6 Thermal conductivity measurement and stretching test with the varying number of layers. (a) In-plane and cross-plane thermal conductivity of anisotropic thermally conductive elastomer with the increasing number of silver plate layers. Compared with the in-plane thermal conductivity, the cross-plane thermal conductivity is relatively lower, but it also enhances the device performance considerably by improving the heat transfer from the junction of the thermoelectric pellet to the outer surface of the device. (b) Based on this result, numerical simulation was conducted in identical conditions to figure 3.4. (c) Stretchability test result for validating the adaptability of human skin.

demonstrates the stretchability test result that was conducted before verifying the analytic results with the experimental result. Even though as the number of layers increased, the result decreased but it showed 6 times higher stretchability with the 3 silver plate layers, and this result implies that can adapt flexibly on human skin.

Compared to the base elastomer, the higher heat dissipation feature of HTCE serves to improve both thermal and chromatic uniformity within a pixel presenting a uniform and rapid response as in figure 3.7. To demonstrate the clear distinction with base elastomer, the thermal and chromatic uniformity within a pixel was compared using the IR camera and digital camera during 0.6A current applied for heating, and -1.5A for cooling modes respectively. The snapshots of IR images imply that the pixel made up of HTCE generates a relatively higher thermal uniformity than the one with base elastomer because the high thermal conductivity of HTCE spreads the heat uniformly throughout the pixel. Notably, during the experiment time of about 80 seconds, each HTCE pixel maintained the high-temperature uniformity, whereas the uniformity state of the base elastomer varied irregularly. This nature of HTCE has great importance in cloaking applications since the disorder of thermal uniformity in pixels might be caused by the malfunctioning of the entire system.

Figure 3.7b and c, as a supporting information, displayed the quantitative temperature difference between the two conditions of HTCE and base elastomer by comparing the temperature standard deviation of the entire unit-pixel area for every 10 s after the electrical current was applied. For the sample with base elastomer, the temperature standard deviation for both heating and cooling modes escalated to 3.8℃ and 3.1℃ respectively, after 80s current was applied. On the other hand, for HTCE, the temperature standard deviation was maintained between 1.7 and 1.5℃

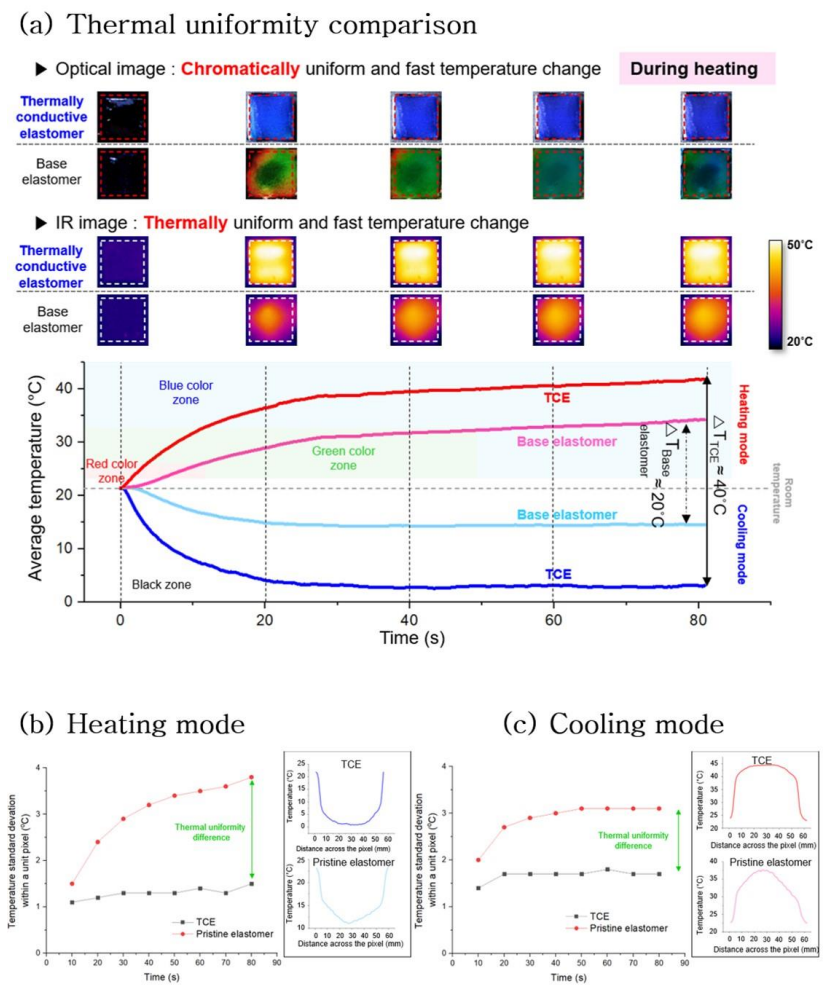

Figure 3- 7 The experiment result of the device performance in perspective of thermal uniformity. (a) Comparison between highly thermally conductive elastomer and base elastomer on the thermal/chromatic uniformity of the unit device pixel and the device performance. Note that the use of the highly thermally conductive elastomer generates high chromatic and thermal uniformity within the pixel while the base elastomer does not. The highly thermally conductive elastomer also serves to enhance the device performance in producing maximum △T. (b) Transient temperature standard deviation within a unit pixel after every 10s for heating and (c) cooling mode.

for heating and cooling modes, indicating the impact of thermal conductivity of HTCE to achieve temperature uniformity within the pixel. Because to express the multispectral cloaking of both visible and IR regions, thermal uniformity plays an essential role in displaying several distinctive color zones with different temperature ranges, HTCE has great importance in this system.

At the IR snapshots on the 2nd zone (at 20 seconds after), several blended colors (the dark green color gradation at the center and the reddish color toward the edge) appear on the pixel with the base

elastomer despite only the blue color being expected to be displayed, whereas HTCE pixel demonstrates expected blue color throughout the entire pixel with high uniformity. The heat mainly generates (or absorbs for the cooling mode) on the junction surface between the Bi2Te3 pellet, copper electrode, and solder. The experiment results indicate the high thermal conductivity of HTCE serves an essential role in processing through the material and structural system for rapid thermal conduction to attain uniformity within the pixel. This enables the improvement of the performance of the device to heat up and cool down when compared with the base elastomer since it has a higher thermal conductivity in any direction(the cross-plane and in-plane). Also, on the graphical representation of the average temperature of the pixel, when the equivalent electrical current was applied temperature difference between the heating and cooling mode of the HTCE pixel and one with the base elastomer was measured as $\Delta THTCE \approx 40$ ℃ and ΔT Base $\approx$ 20 ℃ respectively. It is anticipated that the metallic fillers in HTCE lowered the specific heat than that of base elastomer and in general it helps enhance the device performance because it requires less energy to reach the arbitrary temperature.

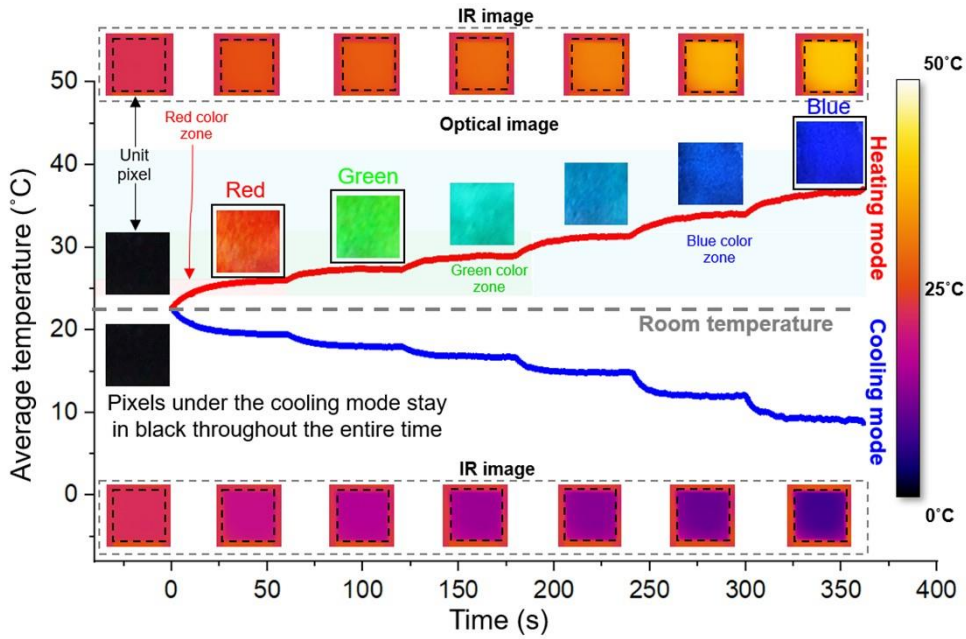

Figure 3- 8 The transient temperature change and its corresponding IR/optical snapshots for the heating and cooling modes at each current increase.

Figure 3.8 shows the IR and optical snapshots of various temperatures according to time for both the heating and cooling modes of the device. The calibrated electrical current was applied to generate the equivalent dT for the heating and cooling modes during the 60s for each step to demonstrate the bi-functional nature of the single device and it showed the high controllability of temperature for a prolonged period to achieve the various target temperature. To express the intended color for an arbitrary amount of time, the pixel temperature must remain within the corresponding temperature zone during the time since each color has a narrow temperature zone for displaying. For this reason, the feature that temperature maintains stably for a prolonged time is a critical factor in articulating colors in the

visible range. The high controllability of temperature for each discrete pixel enables to produce a variety of segmentalized color zone between red and blue such as sky blue or turquoise, expanding the chromatic cloaking application range. Furthermore, this high controllability and stability of pixel temperature are also required for IR cloaking to conceal the human skin temperature into the background. Especially in IR cloaking, the cooling mode of the device conducts a significant role because the human body temperature regulates autonomously and usually to be higher than at room temperature. Therefore, the results not only show that the pixel controllability and sustainability of temperature are demonstrated consistently even under room temperature, but they also enable the artificial skin to thermally cloak the skin temperature into the environment.

Chapter 4

Characterization and Performance Evaluation of Device

4.1 Active Mode for Accurate Thermal Control

In the cloaking system, an active responsiveness that ability of in situ switching from an arbitrary temperature to another is one of the significant prerequisites. However, previous reported wearable thermal electronics are composed of only a single functional heater or cooler, they mainly depend on natural convection which is a very slow heat transfer mode to return to its original state by simply heating up or cooling down so thus it usually takes much longer time to achieve the target temperature. For this reason, the response time and overall performance of the device degrade and limit the potential applications, which is the critical technological shortcoming of thermal devices. Thus, to realize the multispectral camouflageable skin(MCS), the direction and power of electrical current were manipulated(active, variable current, reverse voltage) in cooling and heating modes to attain an arbitrary temperature faster than the existing mode(passive, constant current). Figure 4. 1 shows a distinct difference between an existing low passive mode and a fast active mode in expressing various colors. For instance, to reach the red color zone from the room

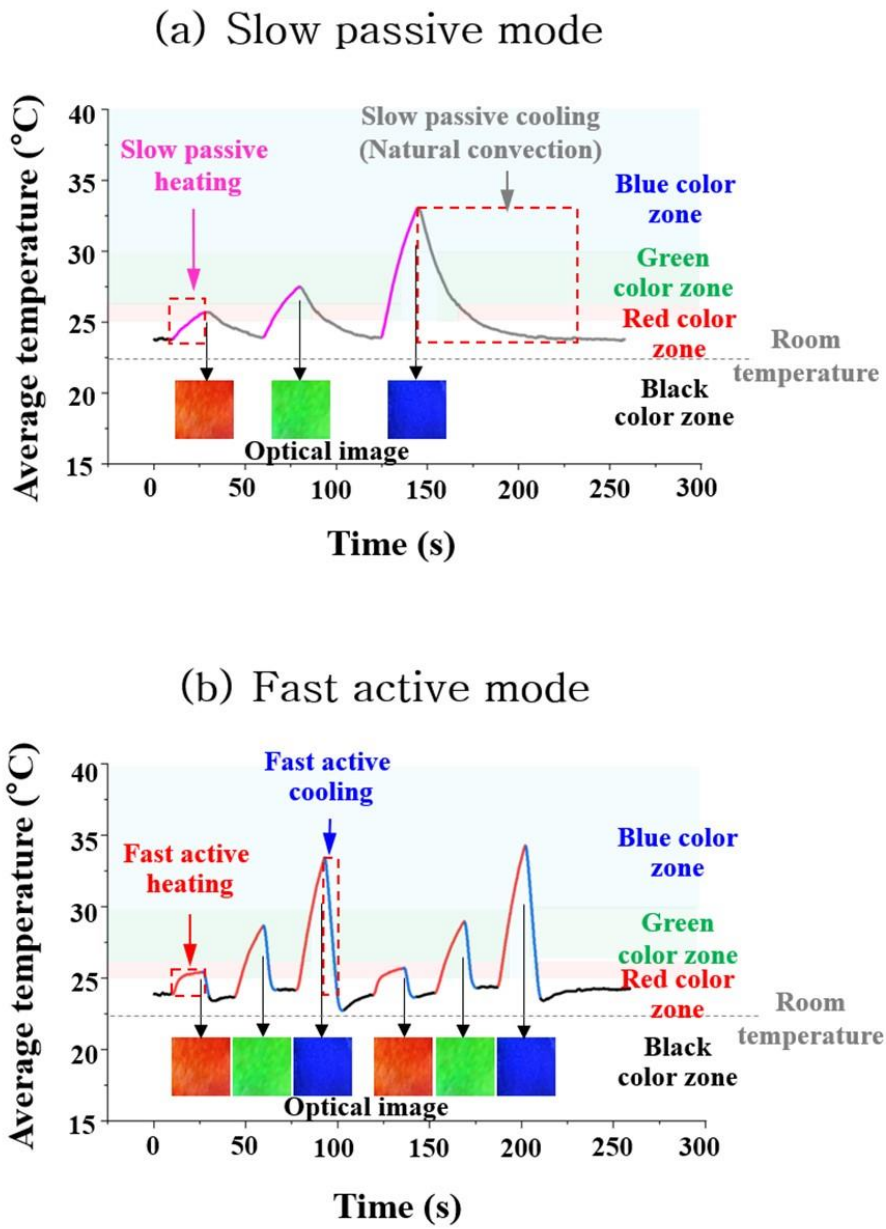

Figure 4- 1 Comparison of thermal response time and controllability between (a) slow passive mode and (b) fast active mode

temperature through the passive mode by applying constant current takes quite a long time because it requires a low electrical current to reach and retain within the red color zone temperature.

To overcome this limitation, the step-wise current was applied as in figure 4.2a and b, first start from high current to quickly heat up to the red color zone and lower down the current to stabilize and remain within the temperature zone. As shown in figure 4.2a, it only took 5.1s to reach the red color zone with fast active heating, while it took almost double of time with the slow passive mode.

Furthermore, whereas previous thermochromic device so far that can only function as an individual heater or cooler has to rely on natural convection to change to the other mode, the bifunctional system studied herein can rapidly approach the target temperature as fast active cooling by applying reverse voltage.

This incomparable feature of the system is extremely appeared in cooling mode as shown in figure 4.3. The result shows that τfast active cooling which is the time it takes to return to room temperature from the blue color zone temperature, was only 6.4 seconds while the passive cooling(natural convection) took almost a minute to reach such temperature. It corresponds to 9.3 times longer than the fast active cooling, finally the fast active mode accomplished approximately 2 color cycles (red-green-blue) during when the slow passive mode was carried out through only one cycle in figure 4.4, and this result validates the applicability to the artificial imperceptible skin, which requires fast response and returning time.

Also, in the IR cloaking mode, the device must be able to cool down to blend into

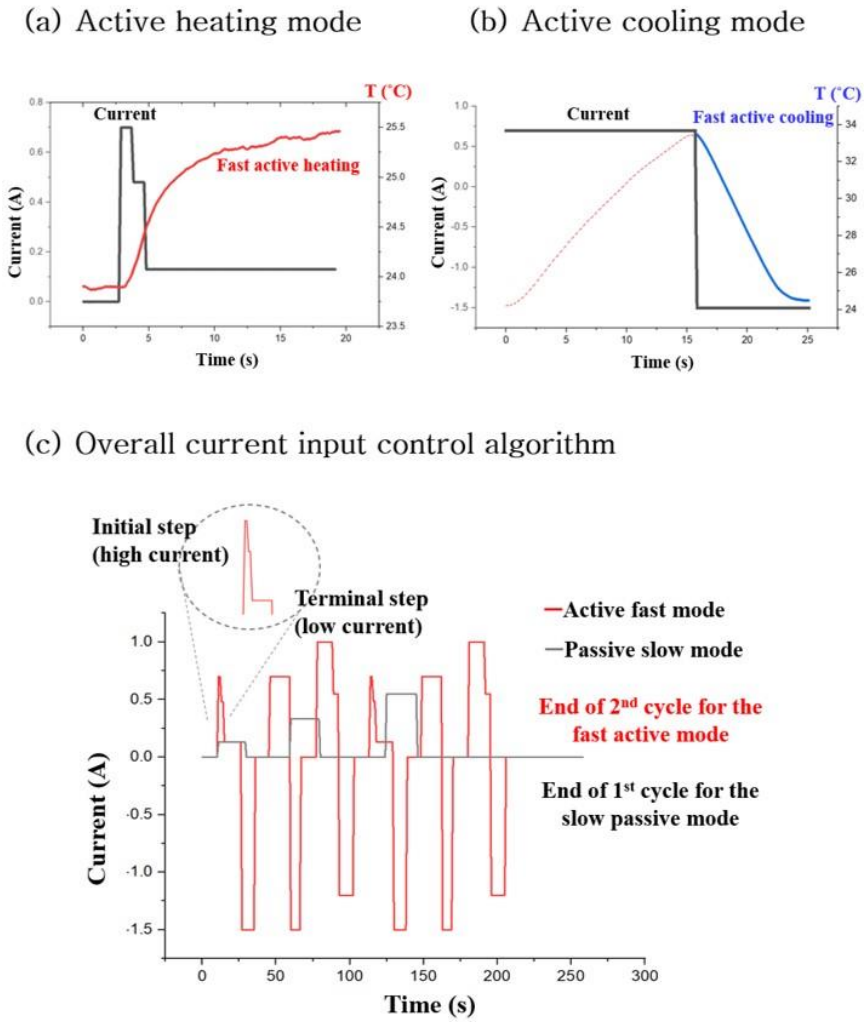

Figure 4- 2 Electrical current change for the fast active mode and passive slow mode. Note that for the fast active mode the electrical current follows a step-wise function to heat up to the target temperature faster and return to room temperature with the cooling mode. (a) input current for (a) fast active heating to reach the red color zone and (b) fast active cooling to return to room temperature from the blue color zone. (c) Overall current input for fast active mode and slow passive mode.

the background temperature quickly since the human body temperature range of 28~32℃ depending upon the body part is usually higher than that of the environment.[18] Therefore, to conceal the skin temperature impeccably from IR radiation detection, the device must achieve the target temperature actively. Figure 4.5 shows the comparison with the simple heating mode by slow passive mode, and the active heating mode as applying abrupt temperature changes by alternating both the cooling and heating process of the device. As a result, the device can rapidly switch from high temperature to low and then to high temperature again based on room temperature because of its bi-functional feature, and this highly significant ability enables the sudden change of the device to the surrounding temperature.

On the other hand, the simple heating mode (or cooling mode) can only heat up(or cool down) in one direction, and it takes long time to saturate until the room temperature, therefore it shows the clear limitation for performing as a cloaking application.

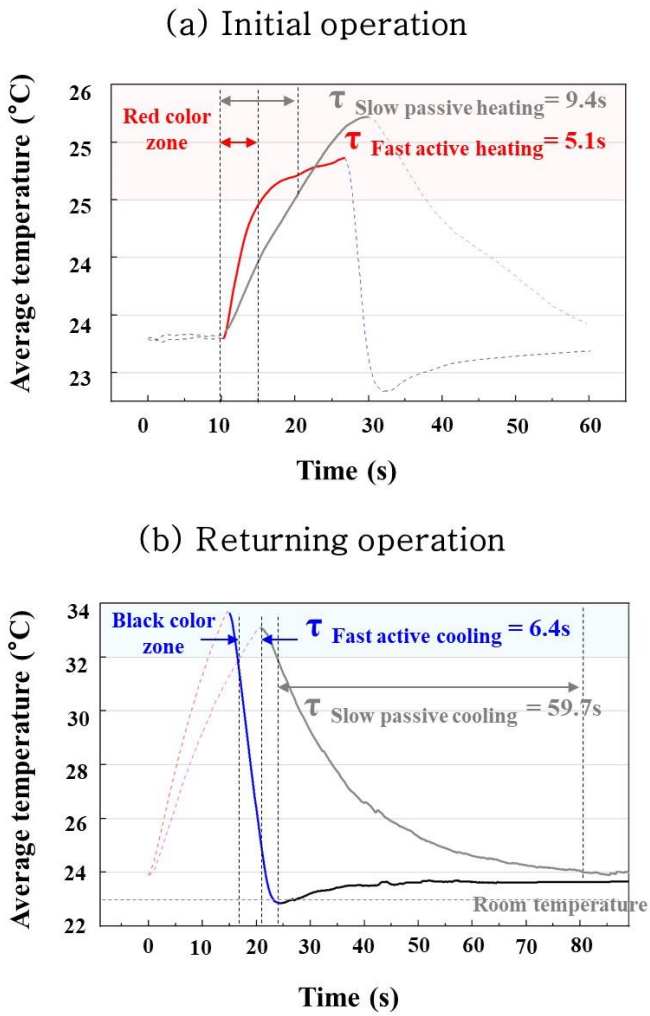

Figure 4- 3 The detail data view of slow passive mode and fast active mode when the device displaying red color in figure 4.1. (a) The magnified initial head and (b) terminating tail regions.

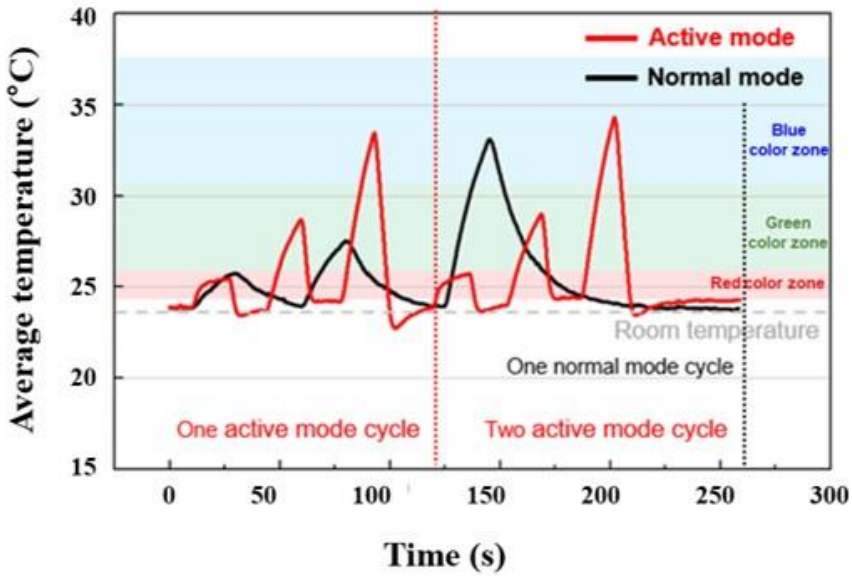

Figure 4- 4 Overlapped graphs of the fast active mode and slow passive mode in cycles to demonstrate the high responsiveness of the fast active mode.

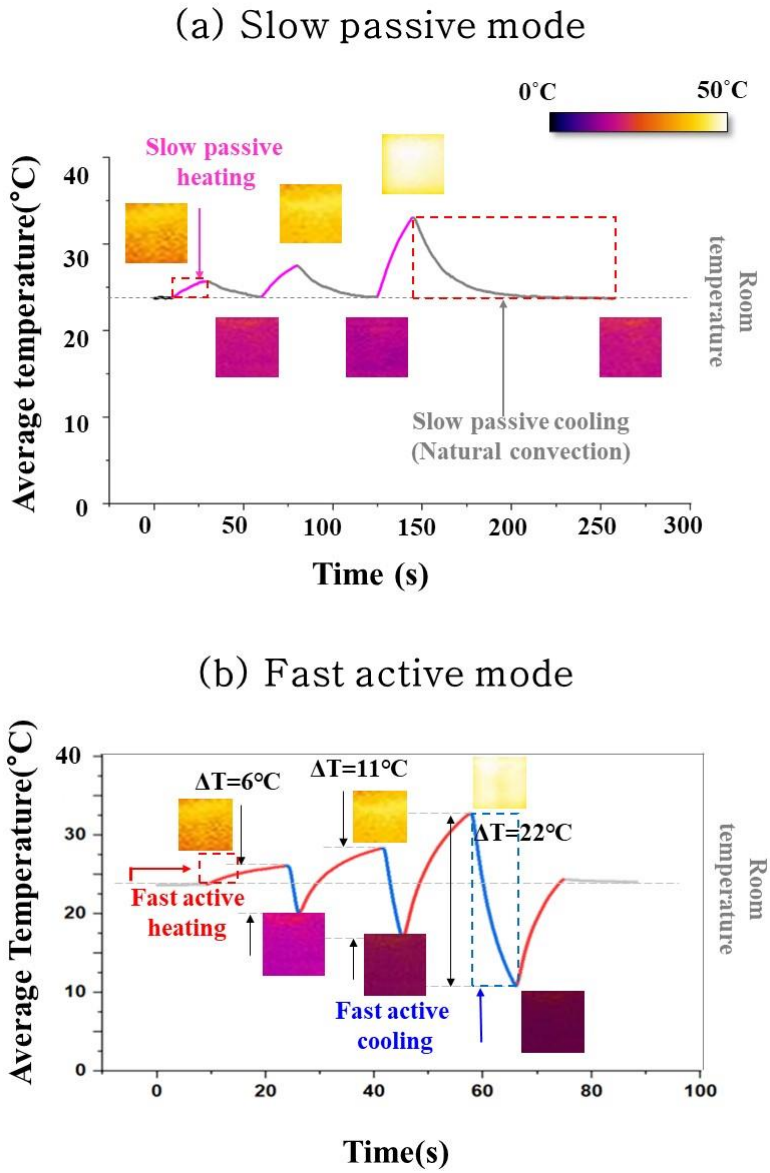

Figure 4- 5 The IR images and temperature comparison on approaching target temperature above and below the room temperature between (a) slow passive mode and (b) fast active mode.

4.2 Mechanical Reliability of the Device against Various Stress

The thermal stability of the device was examined by repeatedly alternating the extreme condition of the cooling and heating mode as shown in figure 4.6. While the device conducting a cloaking application, thermal stress might occur due to the drastic temperature change within seconds at the material interfaces of the device. It possibly is the trigger of an electrical failure of the entire system when the rapid and extreme temperature change operated in numerous cycles. Thus, by alternating the

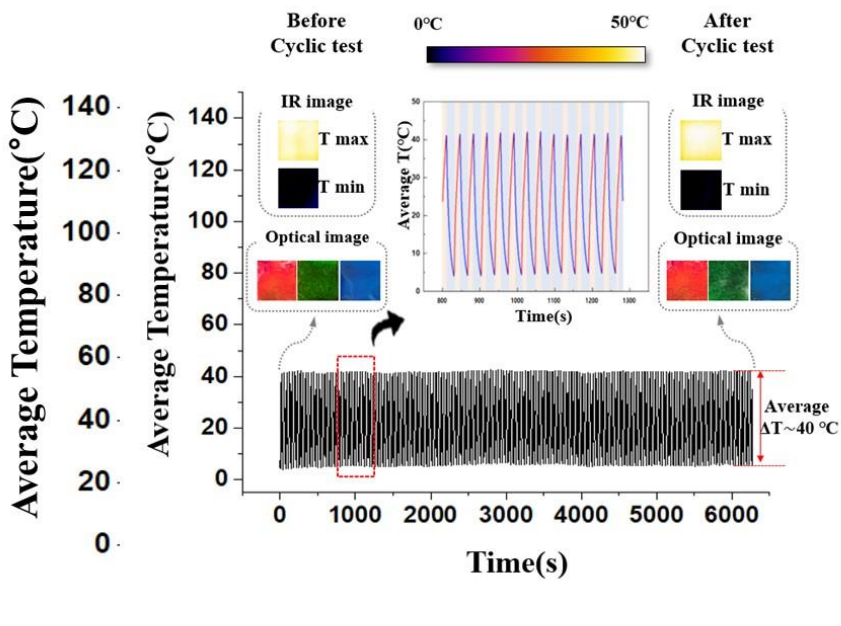

Figure 4- 6 Cyclic temperature change in which cooling and heating modes alternated in cycles with ΔT = 40 °C. Note that the IR and optical images after the cyclic test do not degrade, compared to the ones before the test.

cooling and heating mode with ΔT = 40 °C, the effect of the thermal shock on the device performance was examined in the long-term reliability cyclic test.

Before starting the experiment, the IR and visible (red, green, and blue) images were captured and compared with similar images after lasting more than 6000 seconds. The results demonstrate reliable stability under the frequent temperature

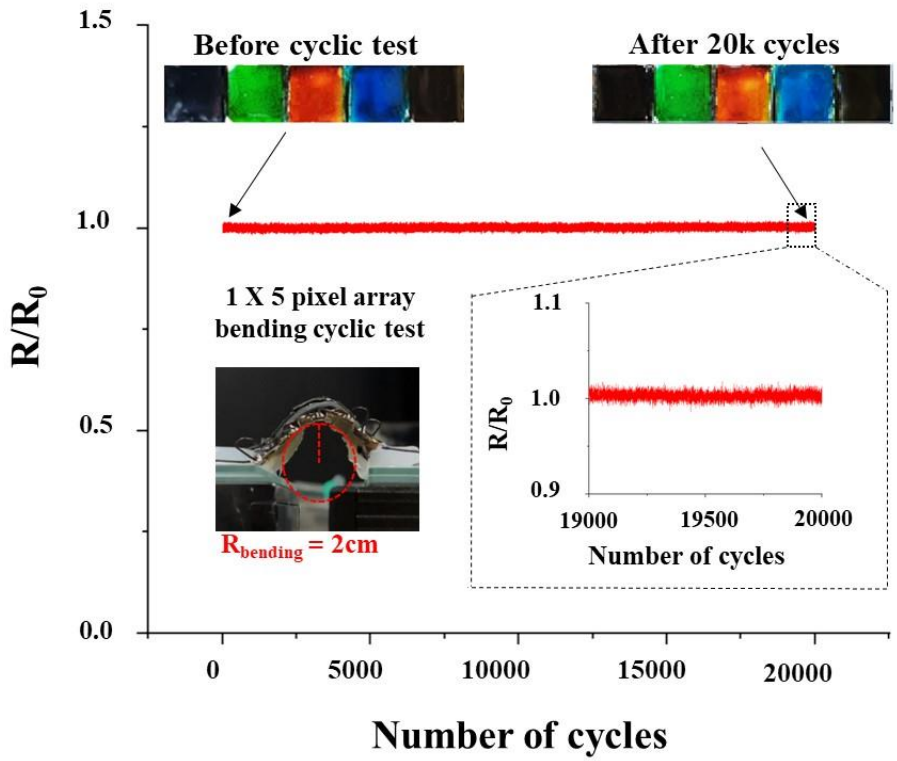

Figure 4- 7 Cyclic bending test during which the 1 × 5 device was repetitively bent while recording electrical resistance to examine the mechanical robustness of the device. Along with constant electrical conductivity, please note that 20 k cycles of bending do not impair chromatic expression of each device pixel.

changes without remarkable performance malfunction or deterioration that is required to realize the cloaking system. Also, for the cloaking device to be fully wearable as artificial skin, its mechanical robustness including electrical connection must be conducted, considering the feature of wearable and flexible electronics because the fatigue stress mainly causes mechanical failure.

Figure 4.7 demonstrates the variation of measured data in resistance ($\frac{R}{R_0}$)during a cyclic test of alternating the folding and unfolding state under flexing the 1 x 5 discrete pixel array with a bending radius of 2 cm. In this test, each pixel (which originally works independently when it turns on as an artificial camouflage device) was connected in series to confirm the stable electrical link. The test was conducted for more than 20000 cycles and during the entire period of the cyclic test, a significantly small electrical resistance changes under 2.43% was observed. It implies the noticeable durability and performance of the flexible artificial skin device against external physical stress in real circumstances. The low modulus of HTCE accomplished the outstanding mechanical stability of the device with strong intermetallic bonding between Cu electrode, thermoelectric pellet, and soldering agents because soft HTCE and thin Cu electrodes play a role to alleviate most of the bending stress, composing a more robust connection of pellets and solders undamaged.

4.3 Visualization Expression based on CIE1931

The author utilized the CIE 1931 RGB graph to define the accurate chromatic profile range created by the device. Figure 4.8 shows the plotted representative RGB colors

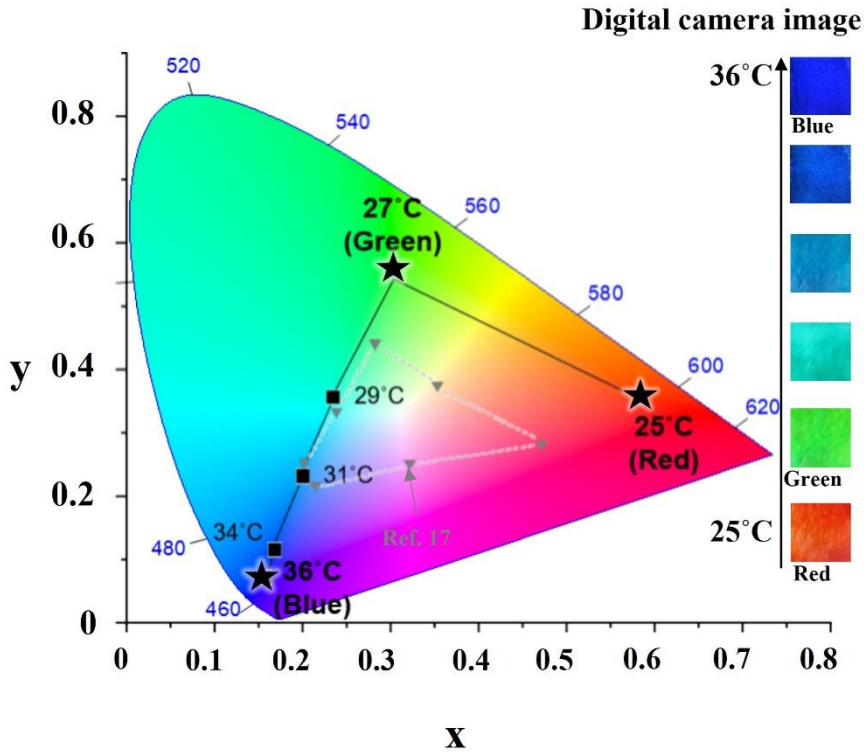

Figure 4- 8 CIE 1931 diagram which maps the discrete colors (indicated as black-star points) expressed with the device at different thermal profiles. The series of the digital camera images correspond to the coordinates on the diagram. The gray dotted lines with flipped triangle points represent the chromatic mapping from another thermochromic device of the recent literature.[21]

of the device in CIE 1931 graph and x-y coordinates were transformed the numerical number correspond to (0.584, 0.369), (0.301, 0.559) and (0.155, 0.0733) respectively. The white-colored line in the middle of the graph implies that most thermochromic devices exhibited a narrow range of colors, the black-colored line of MCS exhibits

a relatively extensive range of colors including RGB with a single thermochromic device by using its highly accurate control of the pixel temperature.

In the following equation($\lambda=n\tilde{}P\cos\theta$), where λ corresponds to the wavelength of the reflected light, n stands for the mean refractive index of the film, P is the helical pitch length, and θ represents the angle between the incident light and the normal to the liquid crystal plane, here the helical pitch length P is depended on the temperature change. The increase in temperature causes the winding of the liquid crystal helix to decrease the spacing between the liquid crystals and then finally reflect light with a shorter wavelength. On the other hand, the unwinding of the liquid crystals helix relaxes the spacing so reflects the longer wavelength and toward the red in the electromagnetic spectrum.[20] This entire thermochromic mechanism is highly reversible and responds rapidly as could be observed in previous figures of this work.

Chapter 5

Thermally Controlled Camouflageable Device

5.1 Contribution of the Thermal Pixels

Exploiting the characterized functions of the device, the final device was composed of an assembly of segmented pixels. To evaluate the feasibility of the device during the experiment, both the digital camera as well as the IR thermal imaging camera were recorded simultaneously. Figure 5.1 demonstrates the photo snapshots, displaying alphabets, A, N, T, and S(in azure blue, green, royal blue, and red respectively) in the visible spectrum and S, N, and U in the IR region (at hot, near room temperature and cold temperature respectively). Pixelization of the device enables the segmentalized operation of the temperature control and thus exhibits an abundant expression of information with a higher degree of freedom. Also, despite each pixel being located adjacently and operated by thermal control, the display of every pixel show clear expression since thermal conduction was not generated between the interface of pixels edge, owing to the thermal engineered design such as figure 5.2b. The high thermal conductivity of developed HTCE herein plays an important role in pixel while at the boundary line, it caused the ambiguous

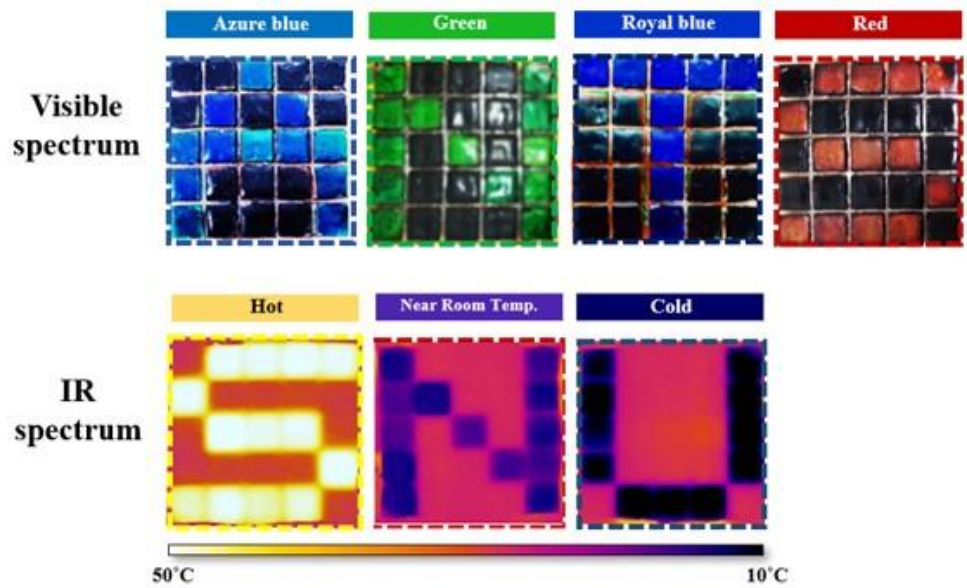

Figure 5- 1 Thermal display displaying visible and IR letters A, N, T in visible colors and S, N, U in various temperature.

temperature interface as in figure 5.2a. Thus, to obstruct the heat transfer between the pixel through the connected HTCE surface, the structure design was developed which has a physically discrete boundary on the surface while maintaining the frame. The thermal display demonstrated above validates its potential in visual controllability and solidifies the foundation for the ultimate aim of this study.

5.2 Multispectral Cloaking Performance

The delicate control of the temperature achieved the bi-functional device with a high degree of flexibility, multiple color expression, pixelized thermal screen, and rapid response time, which satisfies all requirements to be applied as the imperceptible

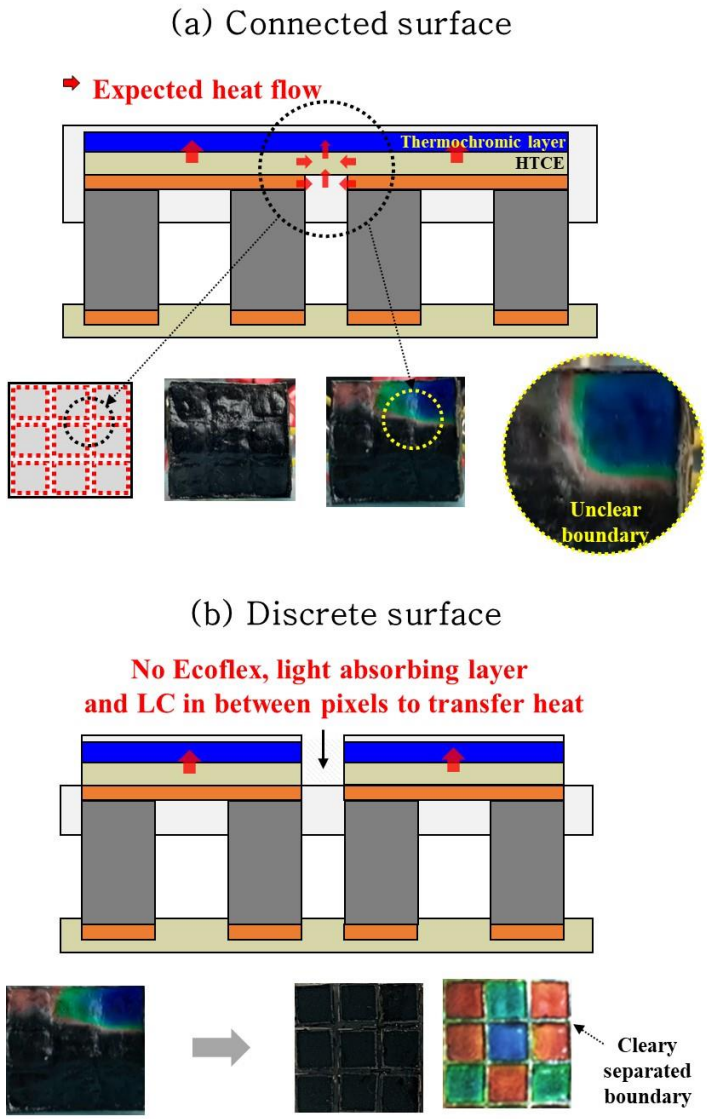

Figure 5- 2 Schematic representation of the two different designs. (a) The polymer materials (HTCE) in between pixels serve to transfer heat and thus possibly result in the undesirable effects such as inaccurate delivery of information or malfunction of the cloaking device. (b) A Completely separated pixel by removing the thermal conduction medium displays a relatively much clear boundary.

artificial skin from the visible to IR bands. To demonstrate the capability of the MCS more intuitively, a virtual map of the several backgrounds which represent the diverse colors, red, green, and blue was prepared as shown in the middle of figure 5.3 and the upper half of the map indicates a cloaking variation in the visible range for day-time. While the other lower half shows the cloaking within the different background temperatures (10 and 50 ℃) for the IR range that exemplifies a night. The device-attached human hand moved across the map, and the individual pixels in the imperceptible artificial skin rapidly adjusted to the background environment with high accuracy that it appears as if there is an empty hole in the hand. The images in the upper half of the map (the maple leaves, grass field, and deep blue ocean) imitated the natural background that we often experience in real life, and the device recreates the comparable background colors red, green, and blue, also, when it across the border of the different background, the device express each background colors concurrently. During the night, since objects can not be easily noticed in the absence of light, the thermographic device is usually utilized to distinguish the homeothermic entities from the dark environment in the military operation. Thus, the lower half of the images likewise, supposing the nocturnal situation, the different temperatures (10, 50℃) represented in the background and functioned as the direct counterpart for the night setting. As shown in the IR part of the images, the pixels in the device autonomously achieve the background temperature as soon as it approaches different thermal sources of the corresponding temperature. In the real situation, the physical environment is composed of a mixture of various color/temperature, so usually the realization of the artificial cloaking system is challenging to mimic a sophisticated background in which various color/temperature exists adjacent to each other. For this reason, to the artificial imperceptible skin, describing the background feature

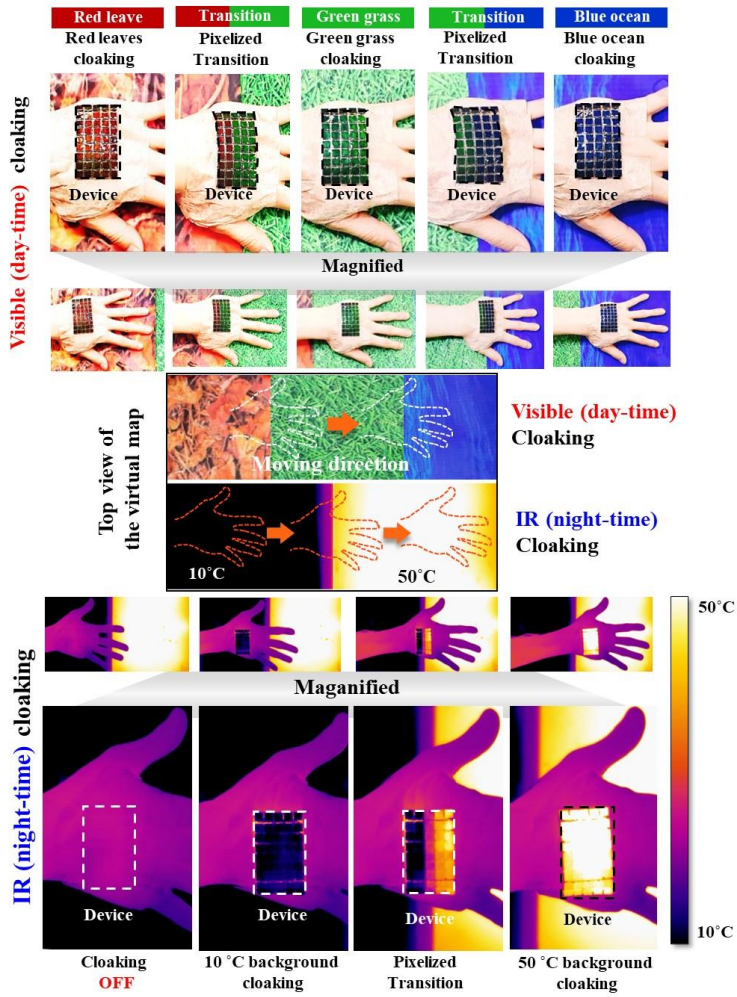

Figure 5- 3 Multispectral cloaking in the visible and IR regimes on the virtual map, in which the device worn on the hand moves across different visible and thermal backgrounds. The background in the visible spectrum consists of red maple leaves, green grass, and deep blue ocean, and the IR backgrounds with different temperature includes 10 and 50 °C. Note that each device pixel can autonomously express different colors/temperatures based on its relative positions as the hand moves across various backgrounds owing to the pixelization of the device.

precisely for both the visible and IR region with quick-adjust to different colors/temperature is highly significant.

Thus, as shown in figure 5.3, the accurate switching of color/temperature based on the corresponding background demonstrates by pixelized conversion from one background to another(for instance from red to green and to blue or 10 to 50℃) as the hand moves across different backgrounds (whether it is a visible or IR mode). Figure 5.3 implies that the developed artificial imperceptible skin in this study is much more challenging to realize thus implying a notable advance, since most of the simple cloaking device that works as an entire system is only capable of generating one color or temperature at a time, while the confluence of individually controlled pixels enables the device to blend into the various background of colors or temperature.

5.3 Active Camouflage Artificial Skin

Finally, to demonstrate the actual cloaking application of the device, it is worn on the human face and observed how it operates in the background of the bushes. The inset of figure 5.4 shows the concentrated images of the cheek to emphasize the effectiveness and wearability of the device. As shown in the figure, during the day(in the visible spectrum) the pixelized device demonstrates its differentiated feature in the cloaking mechanism by generating segmented coloration, which is known to obstruct detection and disrupt perception in nature [23]. This discrete coloration makes the cloaked skin much more difficult to discover so it is utilized as the most

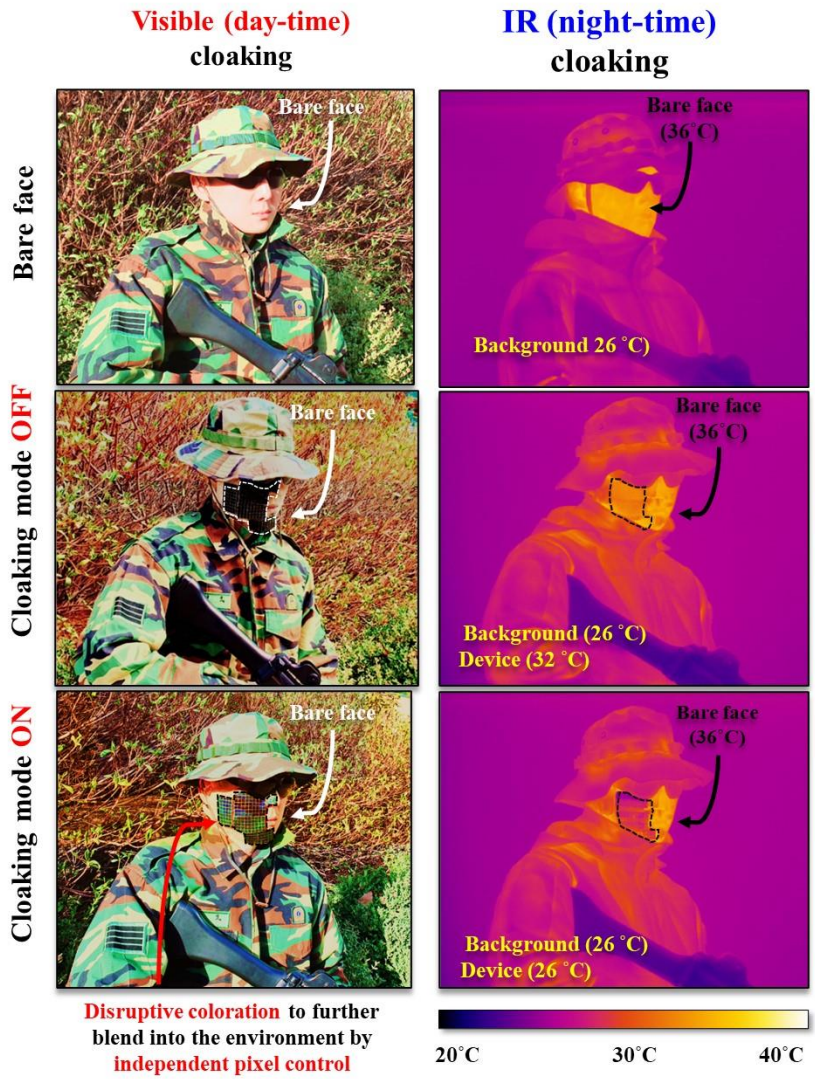

Figure 5- 4 Actual demonstration of multispectral imperceptible artificial skin worn on half of the face for military stealth application. The pixelization of the device allows an autonomous control of each pixel and thus is employed to exemplify disruptive coloration to blend into the environment. In the IR cloaking mode, the device temperature was programmed to approach the background temperature (26 °C), whereas the face temperature stays unchanged (36 °C).

basic and common technique in nature. Considering this mechanism, an electrical current was applied of a specific degree to an appointed region of pixels intentionally, making the human skin hinder to recognize in the forest bushes. As a result, the human face that is covered with the device blended similarly to the background bushes, also matches well with the camouflage-patterned military uniform as if it is a composed part. On the other hand, the bare face without the device is clearly noticeable against the background and uniform with the naked eyes.

Likewise, with the cloaking in the visible spectrum, the device indicates the remarkable capability to cloak the human skin surface thermally when observed by the thermographic camera as well. Since the human body usually controls its temperature to be higher than that of the surrounding environment, the exposed human skin is clearly attracting attention while the device assists the human skin match with the background temperature. This is the reason that the cooling technique which is adapted in this device required as an essential role in thermal cloaking since most of the other thermal cloaking devices can only heat up the temperature, and there are only a few methods to enable both cooling and heating with a single device for wearable application. Thus, in the IR spectrum whereas the imperceptible mode of the device screens the human skin by controlling the temperature to match that of the background, the bare human face is relatively noticeable because of maintaining its temperature as 36℃. Considering most of the previous studies so far, it is highly significant that the entire working wearable device which is developed in this study enables the cloak of the human body actively from the visible to IR spectrum range with high wearability and switchability in a single device, since the existed reported devices only built the fundamental concepts and suggested the prospective potential. [11, 13, 16, 18]

Chapter 6

Conclusion

In summary, inspired by the interesting cloaking system of the cephalopods, the soft and skin-like imperceptive pixelized device was demonstrated with the immediate cloaking ability from visible to IR spectrum by adjusting the thermal operation of the pixel.

Notably, one full-spectrum coverage cloaking system is achieved by integrating each separate cloaking device for the visible and IR range with just simple control of the device temperature, thus displaying that the active multi-spectral cloaking capability is highly comparable to that of cephalopods.

Unlike the previous studies which only suggested the potential of their works in future stealth applications, the skin-like cloaking platform not only imitates the fundamental camouflage features of cephalopods but also presents high practical feasibility for direct usage on the human skin. [5, 11, 13, 14, 15]

The unprecedented features of MCS shown in this study, which provides an entire multispectral cloaking ability with a single device, would contribute significantly to wearable military stealth applications and can also provide a step forward to complete transparency shortly.

REFERENCES

[1] A. Chatterjee, J. A. C. Sanchez, T. Yamuchi, V. Taupin, J. Couvrette, A. A. Gorodetsky, Nature communications, 2020, 11, 2708.

[2] C. Xu, M. C. Escobar, A. A. Gorodetsky, Advanced Materials 2020, 32, 1905717.

[3] P. T. Gonzalez-Bellido, A. T. Scaros, R. T. Hanlon, T. J. Wardill, Iscience, 2018, 1, 24.

[4] H. Ashimoto, M. Goda, R. Futahashi, R. Kelsh, T. Akiyama, Pigments, Pigment Cells and Pigment Patterns, Springer, 2021.

[5] S. A. Morin, S. A. Morin, R. F. Shepherd, S. W. Kwok, A. A. Stokes, A. Nemiroski, G. M. Whitesides, Science 2012, 337, 828.

[6] H. Yi, S.-H. Lee, H. Ko, D. Lee, W.-G. Bae, T.-I. Kim, D. S. Hwang, H. E. Jeong, Adv. Funct. Mater. 2019, 29, 1902720.

[7] D. G. DeMartini, D. V. Krogstad, D. E. Morse, Proc. Natl. Acad. Sci. USA 2013, 110, 2552.

[8] M. D. Bartlett, N. Kazem, M. J. Powell-Palm, X. Huang, W. Sun, J. A. Malen, C. Majigi, PNAS, 2017, 114(9), 2143.

[9] R. Tutika, S. H. Zhou, R. E. Napolitano, M. D. Bartlett, Adv. Funct. Mater. 2018, 28, 1804336.

[10] J. Lee, H. Sul, W. Lee, K. R. Pyun, I. Ha, D. Kim, H. Park, H. Eom, Y. Yoon, J. Jung, D. Lee, S. H. Ko, Advanced Functional Materials, 2020, 30, 1909171.

[11] C. Xu, G. T. Stiubianu, A. A. Gorodetsky, Science, 2018, 359, 1495.

[12] L. Phan, R. Kautz, E. M. Leung, K. L. Naughton, Chem. Mater. 2016, 28, 6804.

[13] G. Wang, X. Chen, S. Liu, C. Wong, S. Chu, ACS Nano, 2016, 10, 1788.

[14] L. Xiao, H. Ma, J. Liu, W. Zhao, Y. Jia, Q. Zhao, K. Liu, Y. Wu, Y. Wei, S. Fan, K. Jiang, Nano Lett., 2015, 15, 8365.

[15] H. Kim, M. Seo, J. W. Kim, D. K. Kwon, S. E. Choi, J. W. Kim, J. M. Myoung, Advanced Functional Materials, 2019, 29, 1901061.

[16] G. H. Lee, T. M. Choi, B. Kim, S. H. Han, J. M. Lee, S. H. Kim, ACS Nano, 2017, 11, 11350.

[17] M. Stevens, S. Merilaita, Philos. Trans. R. Soc., B2009, 364, 481.

[18] Y. Yao, L. M. Keer, M. E. Fine, Intermetallics, 2010, 18, 1603.

[19] K. S. Saladin, Anatomy & Physiology-The Unity of Form and Function, 8th ed., McGraw-Hill, NY, 2018.

[20] S. S. Lee, H. J. Seo, Y. H. Kim, S. H. Kim, Advanced Functional Materials, 2017, 29, 1606894.

[21] R. Hanlon, Curr. Biol., 2007, 17, R400.

[22] K. Hignett, Inspired by Octopuses, This Material Can Hide From Heat Cameras, March, 2018, www.newsweek.com/octopus-cephalopods-infrared-camera-camouflage-866236

[23] R. Gilmore, R. Crook, J. L. Krans, Nat. Educ., 2016, 9, 1.

[24] G. F. Zhao, W. Q. Wang, X. L. Wang, X. K. Xia, C. D. Gu, J. P. Tu, J. Mater. Chem. C2019, 7, 5702.

[25] E. Kavak, C. N. Us, E. Yavuz, A. Kivrak, M. I. Ozkut, Electrochim. Acta 2015, 182, 537.

[26] W. Kang, M. F. Lin, J. Chen, P. S. Lee, Small 2016, 12, 6370.

[27] F. Guo, S. Chen, Z. Chen, H. Luo, Y. Gao, T. Przybilla, E. Spiecker, A. Osvet, K. Forberich, C. J. Brabec, Adv. Opt. Mater. 2015, 3, 1524.

[28] H. Charaya, T. G. La, J. Rieger, H. J. Chung, Adv. Mater. Technol. 2019, 4, 1900327.

[29] J. Kim, K. Han, J. W. Hahn, Sci. Rep. 2017, 7, 6740.

[30] N. Lee, T. Kim, J.-S. Lim, I. Chang, H. H. Cho, ACS Appl. Mater. Interfaces 2019, 11, 21250.

[31] Y. Li, X. Bai, T. Yang, H. Luo, C.-W. Qiu, Nat. Commun. 2018, 9, 273.

[32] S. Hong, S. Shin, R. Chen, Adv. Funct. Mater. 2020, 30, 1909788.

[33] D. Coates, Liq. Cryst. 2015, 42, 653.

[34] C. Kanchanomai, W. Limtrakarn, Y. Mutoh. Mechanics of Materials, 2005, 37, 1166-1174

국문 초록

가시광선-적외선 영역 내 능동 위장을 위한 열전 기반 인공 피부에 관한 연구

두족류는 가장 많은 위장술을 갖고 있는 생물 중 하나로서, 여러가지 기능을 동시에 수행할 수 있는 독특한 능력을 가지고 있어 이를 모방하기 위한 많은 연구가 진행되고 있다. 특히 가시광선과 적외선(IR) 스펙트럼 모두에서 빠른 속도로 능동적으로 배경을 모사할 수 있는데, 온도를 조절하고 동시에 색감을 표현하는 데에 있어 기술적 난제로 남아 있다.

본 연구에서는 하나의 장치로 간단한 온도제어만으로 가시광선부터 IR 스펙트럼까지 주변 환경을 능동적으로 모사할 수 있는 이중 기능 장치를 웨어러블(wearable)한 인공 피부의 형태로 세계 최초로 제작하였다. 펠티어 효과를 이용하여 전류 방향을 통해 냉각과 가열을 조절하면서 외표면 온도를 정확하게 제어하여 IR 스펙트럼에서 열적인 위장을 가능하게 하였다. 이 온도변화는 장치 외표면의 온도 변색 영역에도 작용하여 다양한 색상을 생성하고 제어하는 것을 가능하게 하여 가시광선 스펙트럼 영역까지의 모방의 범위를 확장하였다. 독립적으로 제어될 수 있도록 구성된 픽셀들은 고해상도의 정교한 패턴을 구현하며 장치를 통해 위장 가능한 수준을 한단계 높였다.

즉 하나의 장치로 다중 스펙트럼 내 위장이 가능 한, 웨어러블 장치로서 주-야간 스텔스 기술을 완성하였으며, 이 결과는 차세대 위장 군복 개발 및 다중 스펙트럼 스텔스 기술에 기여할 수 있을 것이다.

주요어: 열전소자
능동위장
가시광선 적외선 스펙트럼
인공피부
생체모방

학 번: 2018-36896